

**DESIGN AND REAL TIME IMPLEMENTATION OF LABVIEW BASED
FRACTIONAL ORDER PID CONTROLLER FOR A MAGNETIC
LEVITATION SYSTEM**

A Thesis
Submitted by

MIDHUN E K
M140337EE

In partial fulfillment for the award of the Degree of

**MASTER OF TECHNOLOGY
IN
ELECTRICAL ENGINEERING
(INSTRUMENTATION AND CONTROL SYSTEMS)**

Under the guidance of
Dr. Sunil Kumar T K



**Department of Electrical Engineering
NATIONAL INSTITUTE OF TECHNOLOGY CALICUT**

NIT Campus P O, Calicut, Kerala, India - 673601.

June 2016

ACKNOWLEDGEMENT

I express my profound sense of gratitude to my project guide, **Dr.Sunil Kumar T K**, Assistant Professor, Electrical Engineering Department for his valuable suggestions, inspiration, support, and continuous encouragement.

I use this opportunity to thank **Prof.Ashok S**, Head of Department, Electrical engineering Department and **Prof.Jeevamma Jacob**, former Head of the Department for providing me with all the necessary facilities for the work.

I would like to thank the my thesis committee: **Prof.Abraham T.Mathew**, **Prof.Vaidyan M.V.** and **Dr.Sunil Kumar T.K.**, not only for their insightful comments and encouragement, but also for the valuable questions which incented me to widen my research perspectives.

I take this opportunity to thank all the other teaching and non teaching staff members of Electrical Engineering Department for their valuable help.

MIDHUN E K

DECLARATION

I hereby declare that this submission is my own work and that, to the best of my knowledge and belief, it contains no material previously published or written by another person nor material which has been accepted for the award of any other degree or diploma of the university or other institute of higher learning, except where due acknowledgement has been made in the text.

Place: NIT Calicut

Signature:

Date:

Name: MIDHUN E K

Reg.No: M140337EE



CERTIFICATE

*This is to certify that the Thesis entitled "**DESIGN AND REAL TIME IMPLEMENTATION OF LABVIEW BASED FRACTIONAL ORDER PID CONTROLLER FOR A MAGNETIC LEVITATION SYSTEM**" is submitted by **Mr. MIDHUN E K** (Roll No M140337EE) to the National Institute of Technology Calicut towards partial fulfillment of the requirements for the award of the Degree of Master of Technology in Electrical Engineering is a bonafide record of the work carried out by him under my supervision and guidance.*

Dr. Sunil Kumar T K

(Guide)

Asst Professor

EED, NIT Calicut

Thesis attested by :

Dr. ASHOK S

Professor

Head of Department

EED, NIT Calicut

Place: NIT Calicut

Date:

ABSTRACT

Fractional Order(FO) PID controller is a generalisation of traditional Integer Order(IO) PID controller using fractional calculus. Fractional order controllers are among the emerging solutions for increasing closed-loop performance and robustness. However, they have been applied mostly to stable processes. When applied to unstable systems, the tuning technique uses the well-known frequency-domain procedures or complex genetic algorithms.

Compared to IO PID controller, the tuning of FO PID controller is more complex and poses several challenges particularly during real time implementation. The fractional order controllers are not widely implemented on the real-time experiments because of the complexity of realization. In this work the tuning and design of FO PID controller based on design specifications such as phase margin, gain cross over frequency and robustness to variation in the gain is proposed. The tuning procedure is given for the general case of a class of unstable systems with pole multiplicity. The advantage of the proposed FO controller consists in the simplicity of the tuning approach. The controllers designed are applied in real time to a Maglev system which is a benchmark system with fast dynamics.

The experimental results provided show that the designed controller can indeed stabilize the magnetic levitation system, as well as robustness against gain variations. The overall control performance, disturbance rejection property and trajectory tracking ability of the system using the proposed controller is validated through experimentation in LabVIEW. For comparison purposes, a simple PID controller is also designed to point out the advantages of using the proposed FO controller. Results demonstrate the effectiveness of FO PID controller over the traditional IO PID controller. Furthermore, the future work of the cooperative motion control system with multi-LabVIEW platforms for fractional order control is introduced briefly.

TABLE OF CONTENTS

	Page
List of Abbreviations	viii
List of Figures	ix
List of Tables	xi

CHAPTERS

1	Introduction	1
1.1	Introduction	1
1.2	Literature Survey	2
1.3	Objective	4
1.4	Organization of the Thesis	4
2	LabVIEW interfaced Magnetic Levitation System	5
2.1	Introduction	5
2.2	System Description	5
2.3	System model	7
2.4	System parameters	9
2.5	Model linearization	9
2.6	Hardware experimental details	10
2.6.1	LabVIEW software system	11
2.6.2	LabVIEW Terminal Board for DAQ	12
2.6.3	Peripheral Feedback Equipments	12
2.7	Summary	12
3	Fractional Order PID Controller	13
3.1	Introduction	13
3.2	Fractional Order PID control design	15
3.2.1	Design specifications	16
3.2.2	Parameter equations based on basic specifications	16
3.2.3	Ranges of λ and μ	18
3.2.4	Determination of the optimal controller	19

3.2.5	Integer Order PID Controller Design	20
3.2.6	Controller Design	20
3.3	Step Response Analysis	21
3.3.1	Simulation Results	21
3.3.2	Experimental Results	23
3.4	Disturbance Rejection	25
3.5	Trajectory Tracking	29
3.5.1	Simulation Result	29
3.5.2	Experimental Result	30
3.6	Robustness Analysis	32
3.6.1	Robustness against Loop gain variation	32
3.6.2	Robustness analysis by considering several operating points	36
3.7	Summary	39
4	Conclusion	40
	REFERENCES	42

LIST OF ABBREVIATIONS

FO	Fractional Order.
IO	Integer Order.
DAQ	Data Acquisition.
FCZ	Fractional Control Zone .
PID	Proportional Integral Derivative.
ISE	Integral Square Error.
IAE	Integral Absolute Error.
LabVIEW	Laboratory Virtual Instrumentation Engineering Workbench
VI	Virtual Instruments.

LIST OF FIGURES

	Page
2.1 Maglev mechanical unit	6
2.2 Maglev control system	6
2.3 Maglev phenomenological model	7
2.4 Free body diagram of Magnetic levitation system	7
2.5 Maglev model for position control	8
2.6 Architecture of LabVIEW experimental platform	10
2.7 LabVIEW front panel	11
3.1 Block diagram of a closed-loop system with fractional-order control actions	14
3.2 Fractional-order PID vs classical PID: from points to plane: (a) integer-order and (b) fractional-order	15
3.3 Block diagram of a closed-loop system with fractional-order controller . .	15
3.4 Bode diagrams of the controller and loop transfer function.(a) Controller (b)loop transfer function and system model	19
3.5 Step response analysis	22
3.6 System step response experimental result with IOPID and FOPID $\omega_c = 24\pi rad/s, \phi_m = 20^0$	23
3.7 System step response experimental result with IOPID and FOPID $\omega_c = 18\pi rad/s, \phi_m = 16^0$	24
3.8 System step response experimental result with IOPID and FOPID $\omega_c = 59\pi rad/s, \phi_m = 40^0$	24
3.9 System disturbance rejection with different $\omega_c s$ by IOPID	25
3.10 System disturbance rejection with different $\omega_c s$ by FOPID	26
3.11 System disturbance rejection with different ϕ_m by IO PID	27
3.12 System disturbance rejection with different ϕ_m by FO PID	28
3.13 Sine wave tracking	29
3.14 Control signal for sine wave tracking	29
3.15 Triangular wave tracking	30

3.16	Control signal for Triangular wave tracking	30
3.17	Sine wave tracking	30
3.18	Control signal for sine wave tracking	31
3.19	Triangular wave tracking	31
3.20	Control signal for triangular wave tracking	31
3.21	Robustness against gain variation by IO PID controller($\omega_c = 24\pi$ and $\phi_m =$ 20 deg)	32
3.22	Robustness against gain variation by FO PID controller($\omega_c = 24\pi$ and $\phi_m = 20$ deg)	32
3.23	Robustness against gain variation by IO PID	34
3.24	Robustness against gain variation by FO PID	35
3.25	Robustness simulation results considering several operating points using IO PID controller	36
3.26	Robustness simulation results considering several operating points using FO PID controller	36
3.27	Robustness experimental results considering several operating points by the IO PID controller	37
3.28	Robustness experimental results considering several operating points by the FO PID controller	37
3.29	Control signals for Robustness analysis by considering several operating points by the IO PID controller	38
3.30	Control signals for Robustness analysis by considering several operating points by the FO PID controller	38

LIST OF TABLES

	Page
2.1 System parameters	9
3.2 Optimal controller parameters for a group of specifications	21

CHAPTER 1

INTRODUCTION

1.1 INTRODUCTION

Nowadays, fractional calculus has been widely used by more and more researchers in many areas of science and engineering. The fractional order controllers have an ability to improve the control performance, and increase the system robustness. Application of fractional calculus is becoming a hot topic in control domain, the fractional order controller design for the classical integer order systems as well as the Fractional order controller design for the fractional order systems. Fractional order calculus appears at the same time with the traditional calculus, which means that the order can be any real number. Compared with the integral order calculus, the fractional order calculus has many advantages: firstly, non-integer order calculus is an extension of classical integer order cases; secondly, the fractional order calculus gives a better description of the systems dynamic performance; thirdly, the fractional order system leads to more adequate modelling and more robust control performance; fourthly, the fractional-order controllers have better disturbance rejection ratios and less sensitivity to plant parameter variations compared with the integral Proportional-Integral-Derivative PID controller. In fractional order PID controller, I and D operations are fractional order, therefore besides setting the proportional, derivative and integral constants K_p , K_i and K_d , one has two more parameters: the order of fractional integration λ and the order of fractional derivative μ . Finding an optimal set of values for a given process (plant) calls for real parameter optimization in five-dimensional hyperspace.

Magnetic levitation principle has wide application in modern engineering world such as High speed Maglev trains and magnetic bearings. Maglev technology minimizes the physical contact between the stationary and moving objects and it reduces the energy loss due to the friction. High speed Maglev trains have already been tested in some places such as Shanghai. The same levitation principle is used in Magnetic Bearings and the main application includes pumps, turbines, fans and other rotating machineries. Maglev system is inherently unstable and non-linear. Also the effect of eddy currents makes the controller design more difficult. By using a traditional integer order PID controller, it is hard to attain a higher closed loop bandwidth and better performance for the magnetic levitation system. Fractional order PID controller is being presented here to attain the above mentioned properties and also to ensure better disturbance rejection property.

1.2 LITERATURE SURVEY

Magnetic levitation systems have received wide attention recently because of their practical importance in many engineering systems such as high-speed Maglev passenger trains, frictionless bearings, levitation of wind tunnel models, vibration isolation of sensitive machinery, levitation of molten metal in induction furnaces, and levitation of metal slabs during manufacturing [1]. In recent years, a lot of research works have been reported for controlling Maglev system. The feedback linearisation method had been used to design controllers for Maglev system [2]-[3]. The input-state, input-output and exact linearisation method were used to design non-linear controllers [4]-[5].

The application of fractional order controller (FOC) has been attracting increased attention in recent years [6]-[10]. In general, the tuning methods for FO PID controllers are classified into analytical, numerical, and rule-based ones [6]. This paper presented a review of tuning methods found in the literature for fractional PID (also known as FPID) controllers. Tuning methods for fractional PIDs found in the literature can be divided into analytical, numerical and rule-based.

In [7], the controller parameters were analytically derived by solving non-linear equations fulfilling the gain/phase crossover frequency and phase/gain margin specifications. Fractional order dynamic model could model various real materials more adequately than integer order and provide a more adequate description of many actual dynamical processes. Fractional order controller is naturally suitable for these fractional order models. In this paper, a fractional order PID controller design method was proposed for a class of fractional order system models.

The robustness to loop gain variations specification proposed in [8] had been widely used to design FO PD and proportional - integral (PI) controllers in [9]. The merits of analytical method are obvious; however, it is available only when the equations are few in number and simple. Therefore, it is very difficult to obtain a complete FO PID controller for the Maglev system by solving five complicated non-linear equations. As for the rule-based method, it can easily calculate the controller parameters based on empirical tuning rules. However, the controlled plant usually should be a system having an S-shaped step response. The Maglev system is open loop unstable; its step response cannot be obtained in the form of open loop, and thus, this method is not suitable.

In comparison, the numerical method is a relatively suitable option of tuning FO PID controllers for the Maglev system in the three cases, which is usually an optimization-based method. In [10], a fractional constrained integral gain optimization algorithm for tuning fractional PI controllers was proposed, in which the controller parameters were obtained by solving an optimization problem with the load disturbance constraint. Considering the complexity of equations, the MATLAB optimization toolbox was adopted to solve this problem. However, the sensitivity and complementary sensitivity functions of the Maglev system in this brief are complicated and the success of this method relies heavily on initial starting values, it is therefore very difficult to solve the non-linear optimization problem.

In [11] a new numerical search tuning method was introduced for a fractional order solid core Magnetic Bearing system, presented the detailed tuning procedures of a numerical search method for the FO PID controller. In practice, high-frequency noises have a strong effect on control performance of the MB (magnetic bearing), and thus, an FO PID controller with a low-pass filter was used in [11]. Compared with the previous numerical tuning methods, this method decreases the difficulty in solving the non-linear optimization problem.

A comparative study on design and tuning of integer order and fractional order PID controllers were described in [12]. This paper provided the comparative study of Particle Swarm Optimization based tuning of integer and fractional order Proportional-Integral-Derivative (PID) controllers using SIMULINK.

A tuning method of fractional order proportional integral differentiation (FOPID) controller for the fractional order system was discussed in [13]. In this paper, the fractional order proportional integral differentiation controller was designed to improve performance and robustness for a class of fractional order system, which can model many real systems in bioengineering. The obvious advantage of using the designed controller was that it can improve dynamic characteristics of the system.

However, most of the existing works did not consider experimental studies. The highlight of this present work is the real time implementation of Fractional Order (FO) PID controller on Maglev system. Both theoretical and experimental studies for a fractional order controller designed Magnetic Levitation system was reported in [14]. However, the controller designed in this work is different from the one considered in [14]. Also the methodology discussed in this is simple and easy to implement.

1.3 OBJECTIVE

- To design a fractional order PID controller for Magnetic levitation system by a numerical method for getting good performance and stability.
- To validate the designed controller on the real time experimental set up on LabVIEW platform.
- To analyse the results obtained and check the robustness of the designed controller against gain variations and by considering several operating points.

1.4 ORGANIZATION OF THE THESIS

The remaining part of this thesis is organized as follows. System description and modelling is presented in Chapter 2. Chapter 3 details the Fractional Order PID controller design , real time experimental validation of the designed controllers and Robustness analysis. Finally Conclusions and future scope are drawn in Chapter 4.

CHAPTER 2

LABVIEW INTERFACED MAGNETIC LEVITATION SYSTEM

2.1 INTRODUCTION

The Maglev set up serves as a simple model of devices, which are becoming more and more popular in recent years ie, Maglev trains and Magnetic bearings. Maglev trains have been recently tested and some lines are already available as for example in Shanghai. Magnetic bearings are used in turbines for the same reason as Maglev trains are being built, which is low friction in the bearing itself, Already many turbines are used commercially where the rotating shaft is levitated with magnetic flux. Some other magnetic bearings applications include pumps, fans and other rotating machines.

The magnetic levitation systems are appealing for their additional possibility of active vibration damping. This can be done by various control algorithms implementations and without any modifications to the mechanical parts of the whole system. The Magnetic levitation unit allows for the design of different controllers and tests in real time using LabVIEW environment.

2.2 SYSTEM DESCRIPTION

Magnetic levitation system is composed of two main subsystems, viz electrical and mechanical. Apart from these two subsystems an infrared sensor is attached to mechanical subsystem. Maglev mechanical unit is shown in Fig. 2.1. Maglev mechanical subsystem composed of an electromagnet, steel ball and a heat sink. Electrical subsystem composed of a i/o card, adapter cable and analogue interface board which has two AD channels and six DA channels. The analogue interface board is used to transfer measured signal from the system to PC and control signals from PC to system. The current through the coil will controls the position of the ball in the mechanical unit, where as the control voltage determines the coil current in electrical subsystem. Thus the coil voltage controls the ball position indirectly. The entire system is encased in a rectangular enclosure which contains three distinct sections. The upper section contains an electromagnet, made of a solenoid coil with a steel core. The middle section consists of a chamber where the ball suspension takes place. One of the electro magnet poles faces the top of a black post upon which a one inch steel ball rests.

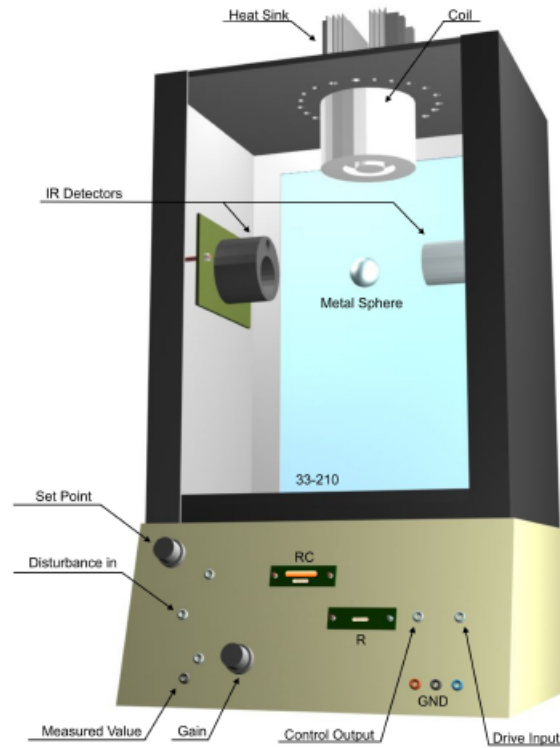


Figure 2.1: Maglev mechanical unit

Apart from the mechanical units, electrical units play an important role in Maglev control. They allow measured signals to be transferred to the PC via an I/O card. The analogue control interface is used to transfer control signals from the PC to Maglev and back. The mechanical and electrical units provide a complete control system set up presented in Fig. 2.2

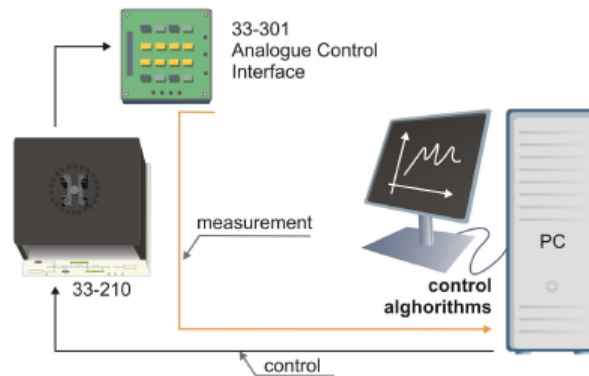


Figure 2.2: Maglev control system

In order to design any control algorithms, one must first understand the physical background behind the process and carry out identification experiments. The next section explains the modelling process of Magnetic levitation

2.3 SYSTEM MODEL

For the design of any controller, the first step involves the analysis of physical background behind the whole process. So plant modelling is the first step in every control project. For the design of controller the Maglev model is shown in Fig. 2.3.

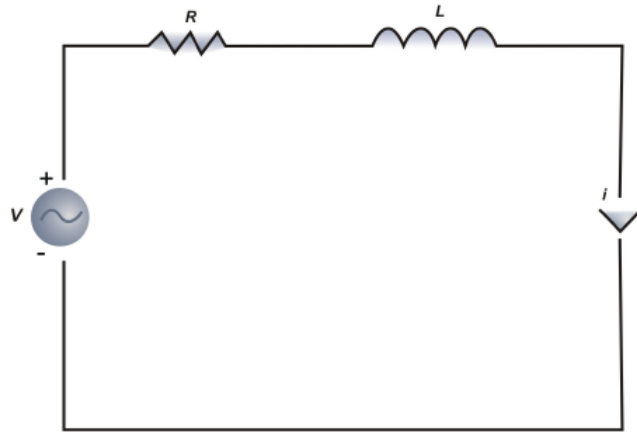


Figure 2.3: Maglev phenomenological model

The Maglev model is non-linear in which coil current (i) and ball distance from the coil (x) are the two system states. In order to design a stabilising controller, the mathematical non-linear model is linearised around the equilibrium point. In addition to this the free body diagram of Magnetic levitation system is given in Fig. 2.4

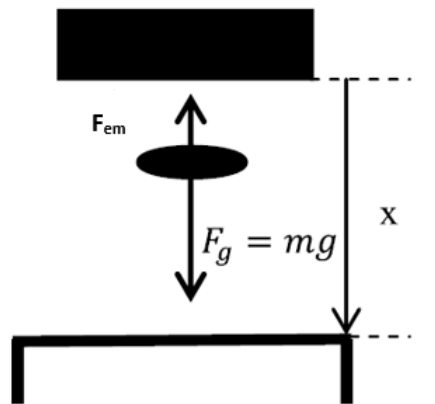


Figure 2.4: Free body diagram of Magnetic levitation system

According to the Maglev system model shown in Fig. 2.3 the non-linear model can be derived as follows, The gravitational force on the ball can be written as:

$$F_g = m_b \cdot g \quad (2.1)$$

where m_b is the mass of the steel ball [kg], $g = 9.81$ is the gravitational speed constant [m/s^2], The force generated by the electromagnet (levitation force) can be written as:

$$F_{em} = -k_1 \frac{i^2}{x^2} \quad (2.2)$$

Where x is the distance [m], \ddot{x} is the acceleration of the permanent magnet [m/s^2] and k_1 is the constant depends on electromagnet parameters (magnetic force constant). The total force experienced by steel ball is given by:

$$F_g + F_{em} = m_b \cdot g - k_1 \frac{i^2}{x^2} \quad (2.3)$$

By Newton's law, the non-linear model can be obtained as follows:

$$\begin{aligned} m_b \cdot \ddot{x} &= F_g + F_{em} \\ m_b \cdot \ddot{x} &= m_b \cdot g - k_1 \frac{i^2}{x^2} \end{aligned} \quad (2.4)$$

To present the full phenomenological model, a relation between the control voltage u and the coil current would have to be introduced analysing the whole Maglev circuitry. However Maglev is equipped with an inner control loop providing a current proportional to the control voltage that is generated for control purposes. The relation among the coil current and control voltage is given by:

$$i = k_2 \cdot u \quad (2.5)$$

The equations 2.4 and 2.5 constitute the non-linear model. Here the control signal is bounded as $[-5V \text{ to } +5V]$ Maglev is a single input single output plant (Fig. 2.5). Position is the output and voltage is the control signal.



Figure 2.5: Maglev model for position control

2.4 SYSTEM PARAMETERS

The system parameters are shown in Table. 2.1 [15].

TABLE 2.1: System parameters

Symbol	Description	Value
L_c	Coil inductance	$412.5mH$
R_c	Coil Resistance	$10ohm$
N_c	No of turns in the coil	2450
L_c	coil length	$0.0825m$
r_c	Coil steel core radius	$0.008m$
R_s	Current sense resistance	$1ohm$
K_m	Electromagnet force constant	$6.5308 * 10^{-5} Nm^2/A^2$
r_b	steel ball radius	$1.27 * 10^{-2} m$
M_b	Steel ball mass	$0.021kg$
K_b	Ball position sensor sensitivity	$2.83 * 10^{-3} m/V$
g	Gravitational constant	$9.81 m/s^2$

2.5 MODEL LINEARIZATION

To carry out the design of linear controller, the non-linear plant is linearised about an equilibrium point, the point at which the system will converge as time tends to infinity. The non-linear system equations are linearised around the operating point of $x_0 = 1.54[cm]$ (the position expressed in volts), $u_0 = 2.56[V]$.

From the equation 2.4

$$\ddot{x} = g - f(u, x) \quad (2.6)$$

$$f(u, x) = k \frac{u^2}{m_b x^2} \quad (2.7)$$

equilibrium point can be evaluated from

$$g - f(u, x) = 0 \rightarrow u_0, x_0 \quad (2.8)$$

By linearisation

$$\ddot{x} = -\frac{\partial f(u, x)}{\partial u} \cdot \Delta u - \frac{\partial f(u, x)}{\partial x} \cdot \Delta x \Big|_{u_0, x_0} \quad (2.9)$$

For the electromagnetic subsystem, the relation between the voltage and the current in 2.5 is used, leading to the final transfer function for the magnetic levitation system.

Applying Laplace transform to the linearised 2.9 leads to

$$s^2 \Delta X = -K_t \Delta u + K_x \Delta X \quad (2.10)$$

$$\Delta X(s^2 - K_x) = -K_t \Delta U \quad (2.11)$$

which leads to the final transfer function

$$\frac{\Delta X(s)}{\Delta U(s)} = \frac{-K_t}{s^2 - K_x} \quad (2.12)$$

where $K_t = 2mg/u_0$ and $K_x = 2mg/x_0$

The open loop transfer function of a Maglev system is a type zero, second order system. The two open loop poles of the system are located at $s = \pm\sqrt{K_t}$ which indicates that the open loop system is unstable due to location of poles on the right half of the s plane.

By substituting the parameter values as $m_b = 0.021kg$, $x_0 = 1.54cm$, $u_0 = 2.56v$, $g = 9.81m/s^2$, Plant transfer function is obtained as:

$$P(s) = \frac{\Delta X(s)}{\Delta U(s)} = \frac{-16.0945}{0.021s^2 - 26.7545} \quad (2.13)$$

2.6 HARDWARE EXPERIMENTAL DETAILS

The LabVIEW interfaced hardware system consists of LabVIEW software, DAQ (Data acquisition) card, and peripheral Feedback equipments. The LabVIEW experimental platform is shown in Fig. 2.6.



Figure 2.6: Architecture of LabVIEW experimental platform

2.6.1 LabVIEW software system

LabVIEW(Laboratory Virtual Instrumentation Engineering Workbench) is a platform and development environment for a visual programming language named ‘G’. ‘G’ is a programming language that uses icons instead of lines of scripts to create applications. In contrast to script – based programming languages, where instructions determine program execution, LabVIEW uses data flow programming. The programs are called Virtual Instruments(VIs), because their appearance and operation can imitate actual instruments, such as oscilloscope, multimeters and so on. The VIs contain three components: the front panel, the block diagram and the icon/connector. The front panel serves as the user interface to control the parameters and indicate the unit step response of the system. We need to manipulate the parameters and indicators to get the the waveform of the unit step response, so we create the LabVIEW user interface in the front panel. The front panel for the real time experiment is shown in fig. 2.7.

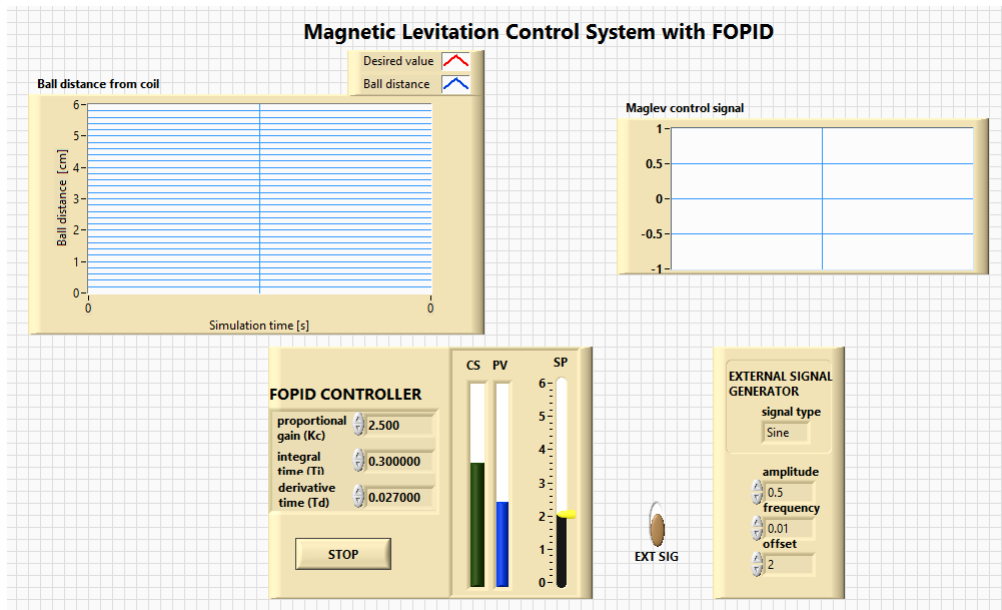


Figure 2.7: LabVIEW front panel

Block diagram contains the graphical code of the VI and the front panel objects appear as terminals on the block diagram. The icon/connectors panel is used to represent the VI in the block diagrams of other objects. In LabVIEW system, the control design and simulation module integrate system simulation and real time implementation, which is a block diagram based environment for simulation of linear and non linear continuous time and discrete time dynamic systems. With the LabVIEW simulation module, one can investigate the time dependent behaviour of complex engineering system, model and

simulate any system that differential and difference equation can characterize. Meanwhile, LabVIEW provides some tool kits to accomplish some complex algorithms.

2.6.2 LabVIEW Terminal Board for DAQ

The plug in hardware for data acquisition (DAQ) as the LabVIEW terminal board was developed by Feedback Instruments. The DAQ terminal board is connected to the computer allowing the user to retrieve digitized data values. With the DAQ terminal board, the hardware only converts the incoming signal into a digital signal that is sent to computer. Because there are many acquisition and analysis functions in LabVIEW, we can use virtual instrumentation to create a customised system for test, measurement, and industrial automation by combining different hardware and software components.

2.6.3 Peripheral Feedback Equipments

The Peripheral Feedback equipments used in the LabVIEW hardware system consists of the Feedback Analogue interface board, Feedback Adaptor cable, Feedback Maglev mechanical unit.

2.7 SUMMARY

The Maglev control aspect covers one area, which is position control. LabVIEW provides various analysis methods for linear systems as far as dynamics are concerned (root locus, frequency analysis tools – Bode diagrams, Nyquist plots, pole and zero maps etc). The non linear mathematical model of the plant from fundamental physical laws has been obtained and the non linear equation has been linearised around the equilibrium point using Taylor's series.

CHAPTER 3

FRACTIONAL ORDER PID CONTROLLER

3.1 INTRODUCTION

PID (proportional integral derivative) controllers are the most popular controllers used in industry because of their simplicity, performance robustness, and the availability of many effective and simple tuning methods based on minimum plant model knowledge. Survey has shown that 90% of control loops are of PI or PID structures. In control engineering, a dynamic field of research and practice, better performance is constantly demanded; therefore, developing better and simpler control algorithms is a continuing objective.

In the past decade, there has been an increase in research efforts related to fractional calculus and its applications to control theory. Clearly, for closed-loop control systems, there are four situations: (1) integer order (IO) plant with IO controller; (2) IO plant with fractional-order (FO) controller; (3) FO plant with IO controller, and (4) FO plant with FO controller. In control practice, the fractional-order controller is more common, because the plant model may have already been obtained as an integer-order model in the classical sense. From an engineering point of view, improving or optimizing performance is the major concern. Hence, our objective is to apply the fractional-order control (FOC) to enhance the IO (integer order) dynamic system control performance.

With non integer order controllers for integer order plants, there are more flexibilities in adjusting the gain and phase characteristics than using IO controllers. These flexibilities make FO control a powerful tool in designing robust control system with less controller parameters to tune. The key point is that using few tuning knobs, FO controller achieves similar robustness achievable by using very high-order IO controllers.

Starting from the block diagram of Figure 4.1, the effects of the basic control actions of type Ks^μ for $\mu \in [-1, 1]$ will be examined in this section. The basic control actions traditionally considered will be particular cases of this general case, in which:

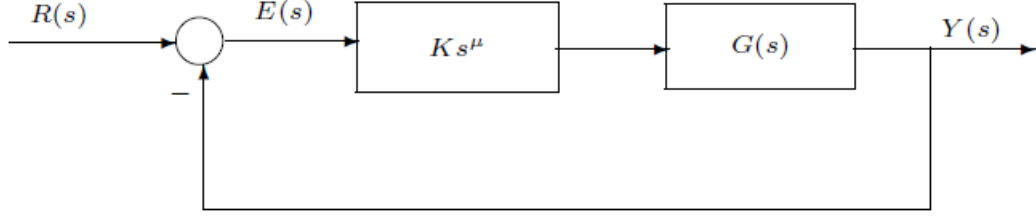


Figure 3.1: Block diagram of a closed-loop system with fractional-order control actions

- $\mu = 0$: proportional action
- $\mu = -1$: integral action
- $\mu = 1$: derivative action

As is known, the main effects of the integral actions are those that make the system slower, decrease its relative stability, and eliminate the steady-state error for inputs for which the system had a finite error. These effects can be observed in the different domains. In the time domain, the effects over the transient response consist of the decrease of the rise time and the increase of the settling time and the overshoot. In the complex plane, the effects of the integral action consist of a displacement of the root locus of the system towards the right half-plane. Finally, in the frequency domain, these effects consist of an increment of $-20dB/dec$ in the slopes of the magnitude curves and a decrement of $\pi/2rad$ in the phase plots.

It is known that the derivative action increases the stability of the system and tends to emphasize the effects of noise at high frequencies. In the time domain, a decrease in the overshoot and the settling time is observed. In the complex plane, the derivative action produces a displacement of the root locus of the system towards the left half-plane. In the frequency domain, this action produces a constant phase lead of $\pi/2$ rad and an increase of $20dB/dec$ in the slopes of the magnitude curves.

The integral-differential equation defining the control action of a fractional order PID controller is given by

$$u(t) = K_p e(t) + K_i D^{-\lambda} e(t) + K_d D^{\mu} e(t) \quad (3.1)$$

Applying Laplace transform to this equation with null initial conditions, the transfer function of the controller can be expressed by

$$C_f(s) = K_p + \frac{K_i}{s^\lambda} + K_d s^\mu \quad (3.2)$$

In a graphical way, the control possibilities using a fractional-order PID controller are shown in fig. 3.2, extending the four control points of the classical PID to the range of control points of the quarter-plane defined by selecting the values of λ and μ .

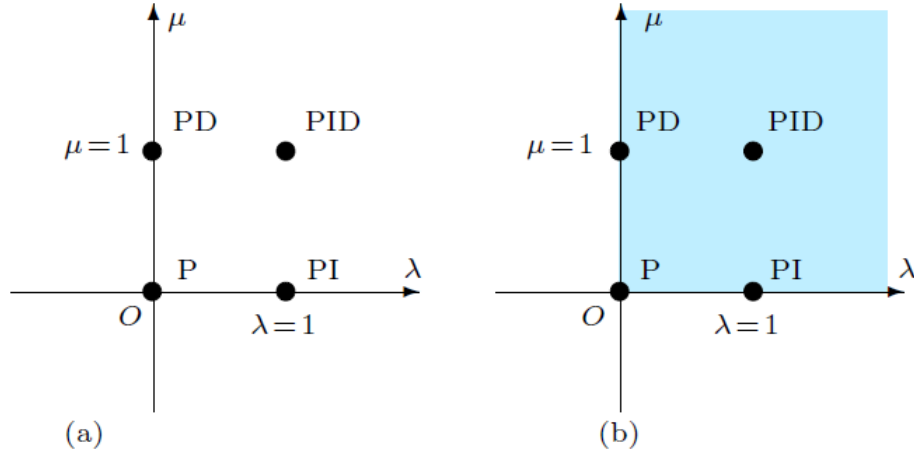


Figure 3.2: Fractional-order PID vs classical PID: from points to plane: (a) integer-order and (b) fractional-order

3.2 FRACTIONAL ORDER PID CONTROL DESIGN

The generalised block diagram of a closed loop system with Fractional Order PID controller is shown in Fig. 3.3.

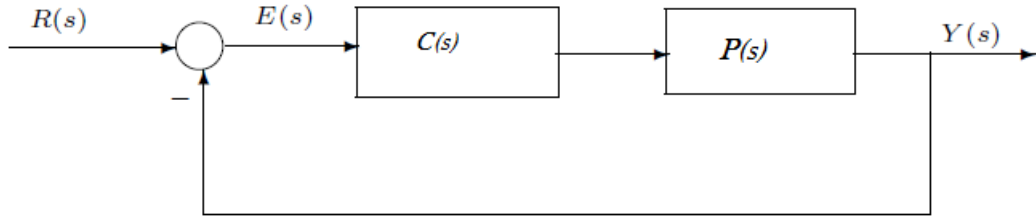


Figure 3.3: Block diagram of a closed-loop system with fractional-order controller

The loop transfer function with FO PID controller $C(s)$ for the system $P(s)$,

$$G(s) = C(s)P(s)$$

According to the forms of the fractional order systems and the FO PID controller discussed, one can systemically design the controller following the three specifications introduced below.

3.2.1 Design specifications

Assume that the gain crossover frequency is given by ω_c and phase margin is specified by ϕ_m . For the system stability and robustness, three specifications concerned with the phase and the gain of open-loop transfer function as follows

- Phase margin specification

$$\text{Arg}[G(j\omega_c)] = \text{Arg}[C(j\omega_c)P(j\omega_c)] = -\pi + \phi_m \quad (3.3)$$

- The gain specification at the cross over frequency

$$|G(j\omega_c)|_{dB} = |C(j\omega_c)P(j\omega_c)| = 0 \quad (3.4)$$

- Robustness to variation in the gain of the plant demands that the phase derivative w. r. t. the frequency is zero, i.e., the phase Bode plot is flat, at the gain crossover frequency. It means that the system is more robust to gain changes and the overshoots of the response are almost the same.

$$\left. \frac{d\text{Arg}[C(j\omega)P(j\omega)]}{d\omega} \right|_{\omega=\omega_c} = 0 \quad (3.5)$$

3.2.2 Parameter equations based on basic specifications

For general FOPID controller

By Eulers formula [13] $e^{j\theta} = \cos\theta + j\sin\theta$ and setting $s = j\omega$, the frequency response of $C(s)$ is as follows

$$C(j\omega) = K_p + K_i(j\omega)^{-\lambda} + K_d(j\omega)^\mu$$

The phase and gain as follows,

$$\text{Arg}[C(j\omega)] = \tan^{-1}(B/A)$$

where,

$$\begin{aligned} B &= K_d \omega^\mu \sin(\mu\pi/2) - K_i \omega^{-\lambda} \sin(\lambda\pi/2) \\ A &= K_p + K_i \omega^{-\lambda} \cos(\lambda\pi/2) + K_d \omega^\mu \cos(\mu\pi/2) \end{aligned}$$

the frequency response of the plant $P(s)$

$$P(j\omega) = \frac{b_0}{A_0 + jB_0}$$

Gain and phase of the plant

$$\begin{aligned} \text{Arg}[P(j\omega)] &= -\tan^{-1}(B_0/A_0) \\ P(j\omega) &= \frac{b_0}{\sqrt{A_0^2 + B_0^2}} \end{aligned}$$

Then the loop frequency response $G(j\omega)$ is that,

$$G(j\omega) = C(j\omega)p(j\omega)$$

The phase and gain of the open-loop frequency response are as follows,

$$\begin{aligned} \text{Arg}[G(j\omega)] &= \tan^{-1}(B/A) - \tan^{-1}(B_0/A_0) \\ |G(j\omega)| &= |C(j\omega)| |P(j\omega)| = \frac{b_0 \sqrt{A^2 + B^2}}{\sqrt{A_0^2 + B_0^2}} \end{aligned}$$

According to specification (i), the phase of $G(j\omega)$ can be expressed as,

$$\text{Arg}[G(j\omega)] = -\pi + \phi_m \quad (3.6)$$

According to specification (iii) about the robustness to gain variations in the plant,

$$\begin{aligned} \frac{d\text{Arg}[C(j\omega)P(j\omega)]}{d\omega} \Big|_{\omega=\omega_c} &= 0 \\ &= \tan^{-1}(B/A) - \tan^{-1}(B_0/A_0)' = 0 \end{aligned} \quad (3.7)$$

According to specification (ii), we can get,

$$|G(j\omega)| = |C(j\omega_c)| |P(j\omega_c)| = 1 \quad (3.8)$$

3.2.3 Ranges of λ and μ

Based on the previous analysis, the determination of ranges of λ and μ is the key for solving the equations. To simplify the problem, the controller 3.2 is utilized to analyze the relation between the orders and the basic specifications. According to 3.2, the phase of controller is

$$\angle C(j\omega) = \tan^{-1} \left(\frac{K_d \omega^\mu \sin \frac{\mu\pi}{2} - \frac{K_i}{\omega^\lambda} \sin \frac{\lambda\pi}{2}}{K_p + K_d \omega^\mu \cos \frac{\mu\pi}{2} + \frac{K_i}{\omega^\lambda} \cos \frac{\lambda\pi}{2}} \right) \quad (3.9)$$

When the phase is equal to zero, the corresponding frequency, namely, ω_t is calculated as follows:

$$\omega_t = \left(\frac{K_i \sin \frac{\lambda\pi}{2}}{K_d \sin \frac{\mu\pi}{2}} \right)^{\frac{1}{\lambda+\mu}} \quad (3.10)$$

For the FO PID controller in fig. 3.4, only when the crossover frequency ω_c exceeds ω_t , the derivative term can take a leading role and provide the phase compensation for the Maglev system. From 3.9, the maximum phase of the controller is

$$\lim_{\omega \rightarrow \infty} \angle C(j\omega) = \frac{\mu\pi}{2} \quad (3.11)$$

Supposing that the phase of 3.2 and the phase of 2.13 at ω_c are ϕ_f and $-180^\circ - \phi_c$ ($\phi_f > 0$ and $\phi_c > 0$), respectively (Fig. 5), to fulfil the phase specification 3.3, the controller should meet

$$\frac{\mu\pi}{2} > \frac{\phi_f\pi}{2} \geq \frac{(\phi_m + \phi_c)\pi}{180} \quad (3.12)$$

From 3.12, a lower limit of μ can be determined. On the other hand, the gain of the loop transfer function $G(s) = C(s)P(s)$ at ω_c is equal to 0 dB in fig. 3.4. When the frequency exceeds ω_c , the controller gain increases with a slope of 20μ dB/decade. In contrast, the model gain decreases with a slope of -20γ dB/decade [for 2.13, $\gamma = 2$]. Obviously, the gain of $G(s)$ increases with μ . However, too large high frequency gain will amplify noises, and even causes instability, So the gain slope of $G(s)$ should at least be less than zero, that is

$$20\mu - 20\gamma < 0 \quad (3.13)$$

Therefore, a conservative range for μ is $((\phi_m + \phi_c)/90, \gamma)$. As to λ , to eliminate the system steady state error, an integral term is necessary. However, the stability of system will become worse as λ increases, and thus λ also has an upper limit. From fig. 3.4, the integral term in the FO PID controller mainly works in the low frequency band (less than ω_t). However, the three given specifications are not related to the low frequency band, and thus, it is difficult to directly determine the specific upper limit from 3.3 – 3.5. To this end, a relative conservative range of λ is taken as $(0, 2)$.

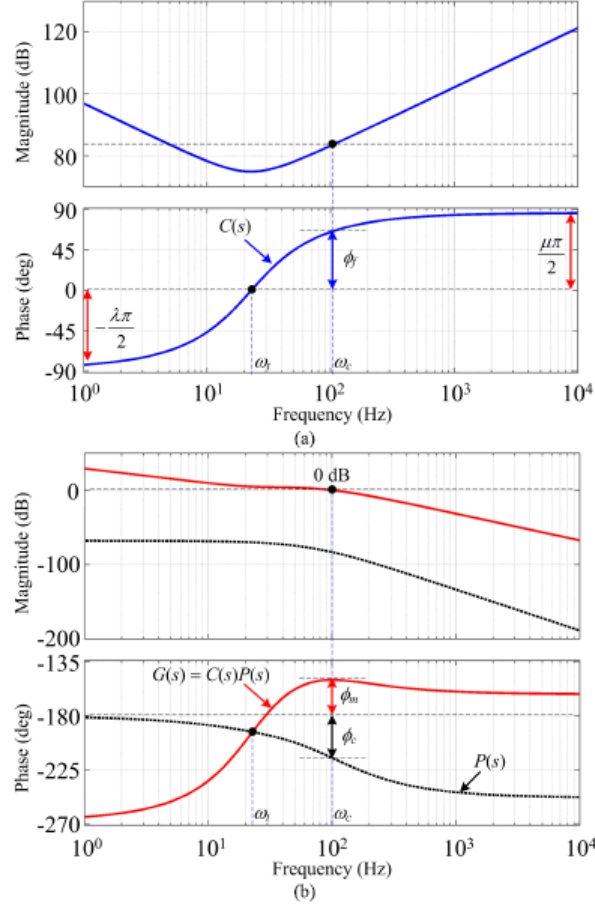


Figure 3.4: Bode diagrams of the controller and loop transfer function. (a) Controller (b) loop transfer function and system model

3.2.4 Determination of the optimal controller

The section presents the determination of the optimal FO PID controller by evaluating exact performance indexes. The basic process is summarized as follows.

- The initial ranges of λ and μ are first calculated based on a group of given specifications and Maglev system model.
- Evaluate the rest of three parameters by solving 3.6, 3.7 and 3.8. At last a series of

- The correctness of the solutions (i.e., K_p , K_i and K_d) are verified by substituting the parameters into design specifications.
- From the unit step response of the closed loop Maglev system, the integral of the absolute error (IAE) is calculated within a limited range (0 to 0.5 sec) for each feasible controller.

$$IAE = \int |e(t)| dt$$

- If the performance of the system with the optimal FO PID controller is satisfactory, the process is ended. otherwise, two narrow intervals that take the λ and μ of the optimal controller as midpoints, respectively, are constructed as the new ranges of λ and μ and then the search step size is reset to a smaller value. The process is repeated from 1) again until the optimal controller for the specified specifications is obtained.
- If the above optimal controller is still not satisfying, a new group of specifications is assigned by qualitative analysis of the relation between specifications and system performance, and then the process is repeated from 1) again; otherwise, it is ended.

3.2.5 Integer Order PID Controller Design

To compare the FO PID and the IO PID controllers, an IO PID controller fulfilling the same specifications is designed.

Let $\lambda = \mu = 1$, the FO PID controller becomes 3.2 becomes an IO PID controller

$$C(s) = K_p + \frac{K_i}{s} + K_d s \quad (3.14)$$

The basic parameter equations 3.6, 3.7 and 3.8 can be simplified to uniquely determine parameters of the controller.

3.2.6 Controller Design

In this section, two categories of controllers based on several groups of specific specifications are designed to stabilize the Maglev system, and the performance comparisons of controllers are also carried out by simulation in next section.

To guarantee that the given specifications are feasible to design 3.2, the FCZ (Feasible Control Zone) of the controller should be probably determined in advance (i.e., the (1)

and (2) parts in the determination of the optimal controller). The FCZ is a set composed of the (ω_c, ϕ_m) specifications that the loop transfer function can stably fulfil.

The IO PID controller is a special case of the FO PID controller 3.2, and thus, the FCZ of IO PID is smaller and included in that of 3.2 due to the flexibility of λ and μ . To this end, only the FCZ of IO PID is determined to reduce the amount of calculation. From the open-loop bandwidth of the Maglev model, the ranges of the (ω_c, ϕ_m) specifications to be calculated are selected as $(10\pi, 25\pi)$ *rad/s* and $(10^\circ, 50^\circ)$, respectively.

Seven groups of feasible basic specifications are selected to design the controllers for performance analysis. Based on this rule, all the optimal controller parameters are presented in Table II.

TABLE 3.2: Optimal controller parameters for a group of specifications

parameters		1st group ($18.8\pi, 16^\circ$)	2nd group ($24\pi, 20^\circ$)	3rd group ($23.14\pi, 30^\circ$)	4th group ($11.59\pi, 40^\circ$)
λ	FO PID	0.596	0.600	0.623	0.688
μ		0.880	0.629	0.897	0.868
K_p		-1.90108	-2.387	-3.2045	-2.442
K_i		-54.06	-48.827	-69.97	-46.23
K_d		-0.1612	-0.481	-0.183	-0.193
K_p	IO PID	-3.14	-3.069	-2.51	-2.574
K_i		-34.625	-38.0693	-8.32	-16.087
K_d		-0.0340	-0.02079	-0.0519	-0.07261

3.3 STEP RESPONSE ANALYSIS

To compare system dynamic performance, the step response simulation for part of designed controllers is implemented

3.3.1 Simulation Results

Since it has already been experimentally modelled the position control system with a transfer function 2.13, first test the simulations in Simulink firstly, then the simulation results can be compared with the real-time experiments on the Maglev system. Thus, the verification of our proposed method is more effective.

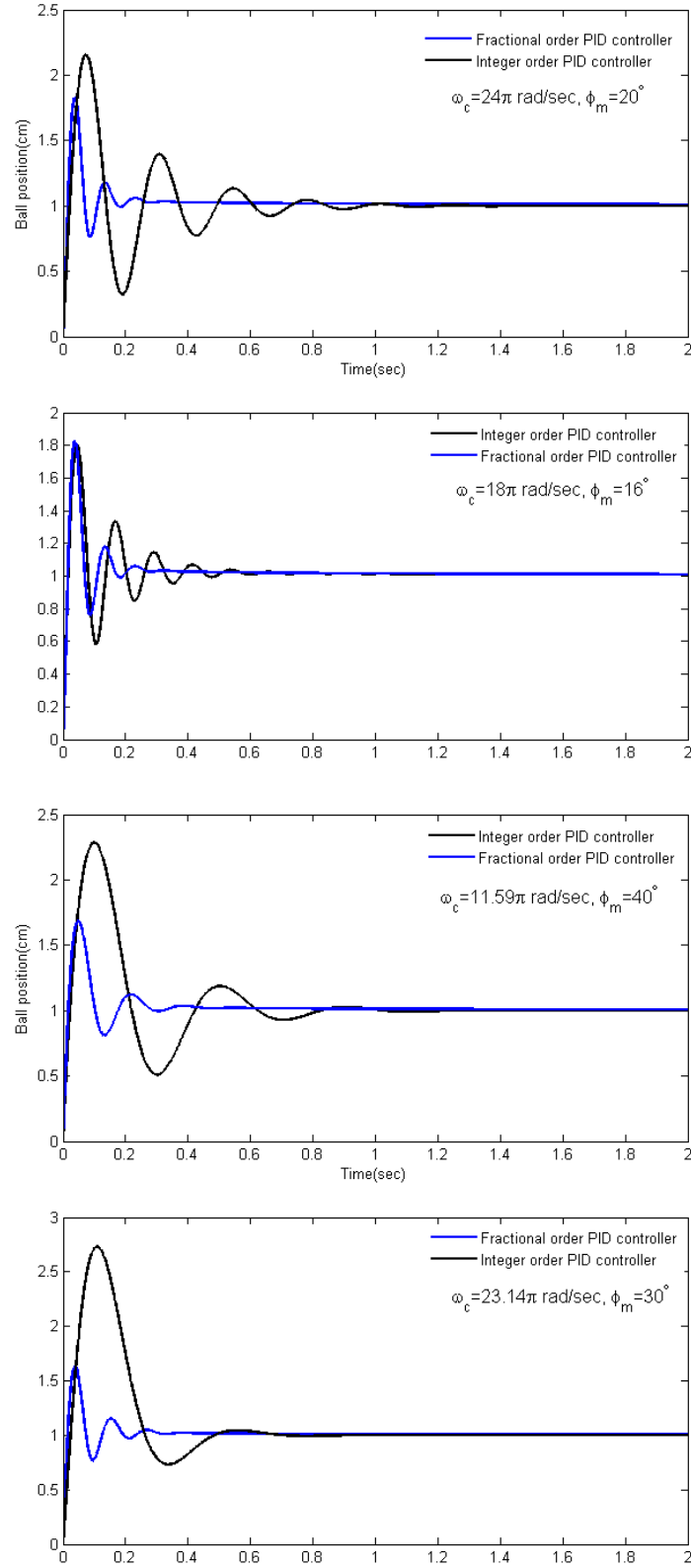


Figure 3.5: Step response analysis

From fig. 3.5, the system with FO PID controllers has more favourable dynamic performance (smaller overshoot, oscillation, and less settling time) than that with the IO PID controllers. In addition, the FO PID controller can help the Maglev system to achieve a larger stability margin and a higher closed-loop bandwidth from the last group of controllers.

3.3.2 Experimental Results

In this phase, the designed controllers are applied to the real Magnetic Levitation system in fig 2.6

For the step response experiments a unit set-point is selected as the reference input. The step response experimental results are shown below. For every step response corresponding control signals are also shown below.

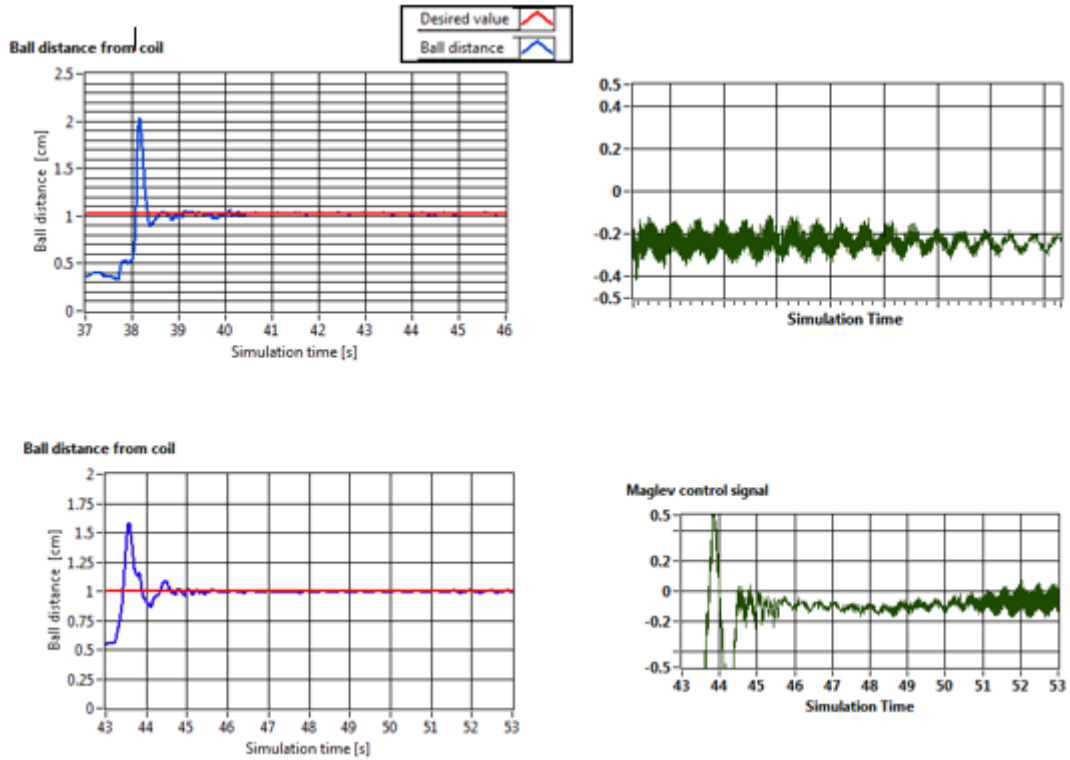


Figure 3.6: System step response experimental result with IOPID and FOPID $\omega_c = 24\pi\text{rad/s}$, $\phi_m = 20^\circ$

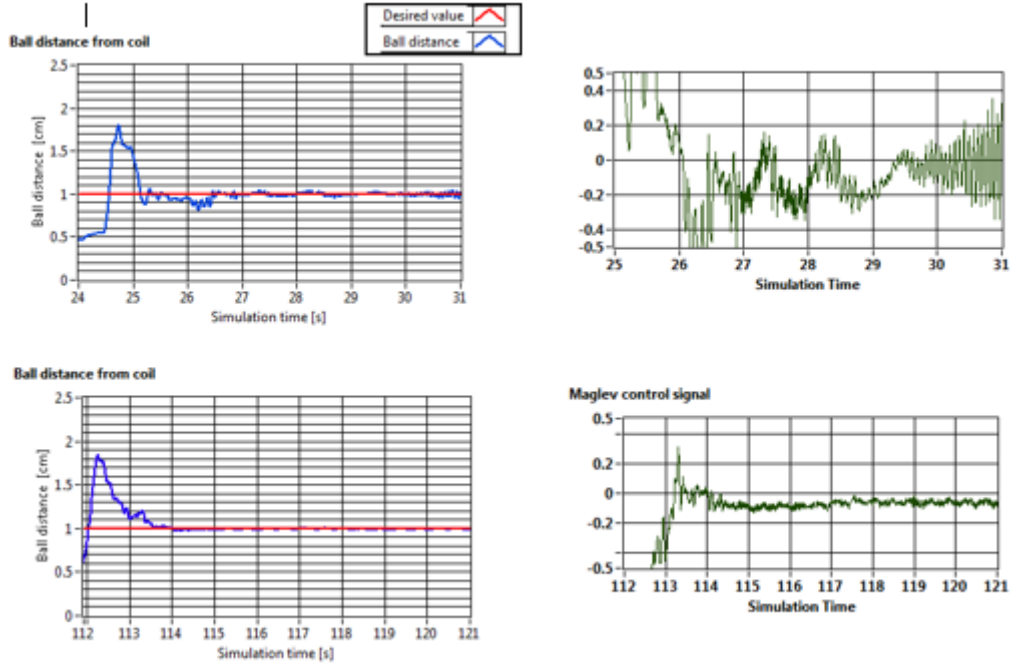


Figure 3.7: System step response experimental result with IOPID and FOPID $\omega_c = 18\pi\text{rad/s}, \phi_m = 16^0$

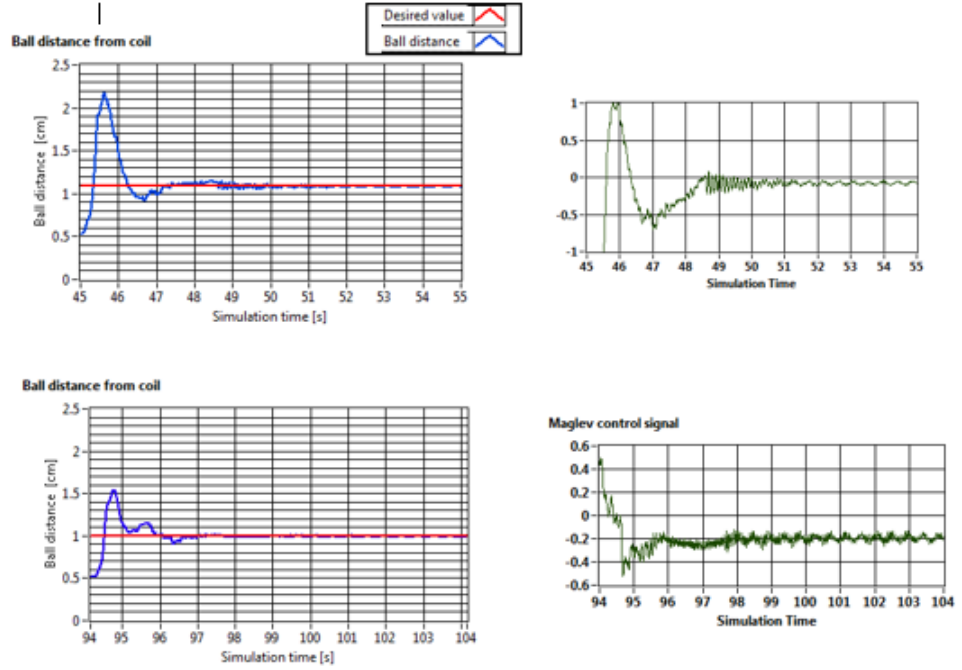


Figure 3.8: System step response experimental result with IOPID and FOPID $\omega_c = 59\pi\text{rad/s}, \phi_m = 40^0$

To compare the system dynamic performance, step response experimental results are collected. From the system step response results, the FO PID controllers have better dynamic control performance (less settling time and small overshoot). In addition to this Maglev system achieve a larger stability margin with the help of designed FO PID controllers. The overshoot can be minimized by increasing phase margin and gain cross over frequency. However when the phase margin and gain cross over frequency is too high the IO PID makes the system unstable.

3.4 DISTURBANCE REJECTION

In this phase disturbance rejection property of fractional order PID is evaluated. A 0.2V pulse is taken as disturbance input which is generated in LabVIEW environment. To study the disturbance rejection property it is first classified into two cases, different phase margin with constant gain cross over frequency and different gain cross over frequency with constant phase margin. The following figures show the experimental results of the disturbance rejection with the ω_c variations.

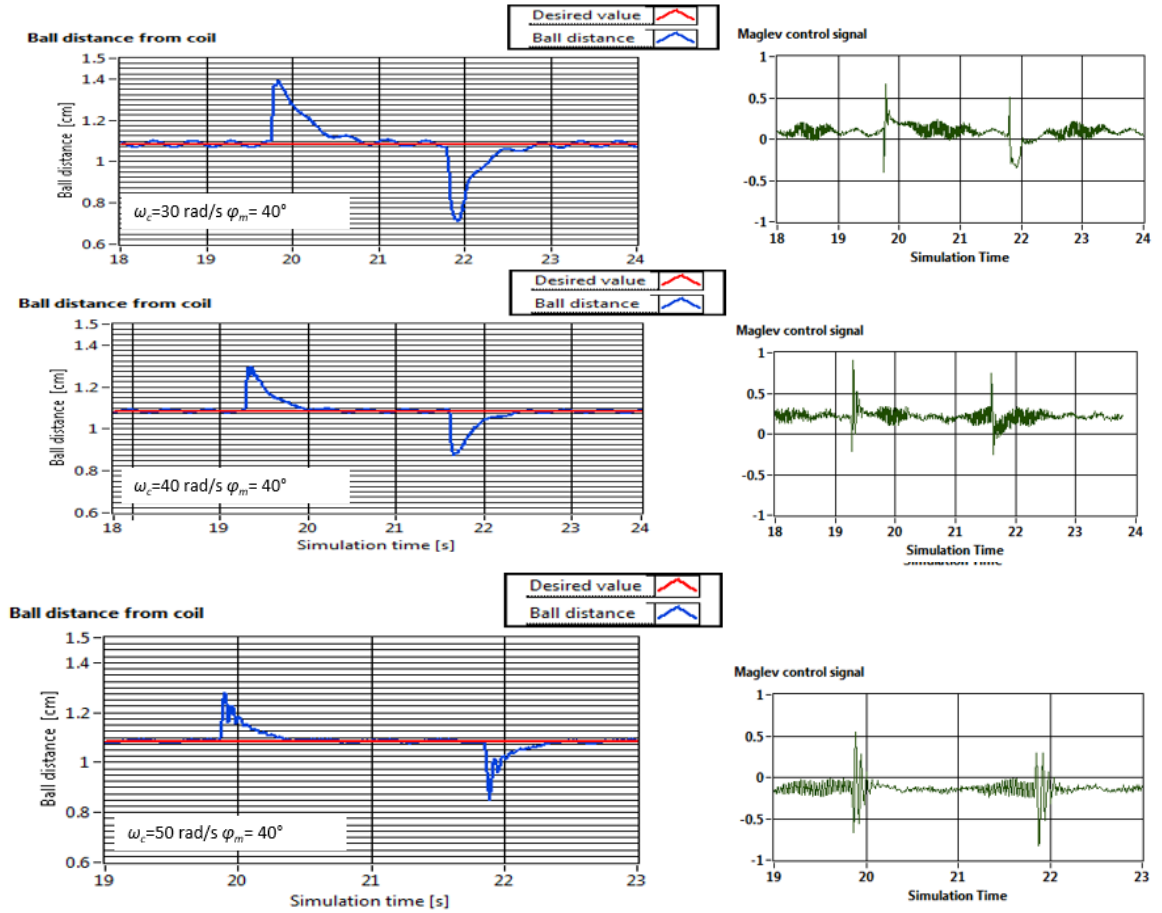


Figure 3.9: System disturbance rejection with different ω_c 's by IOPID

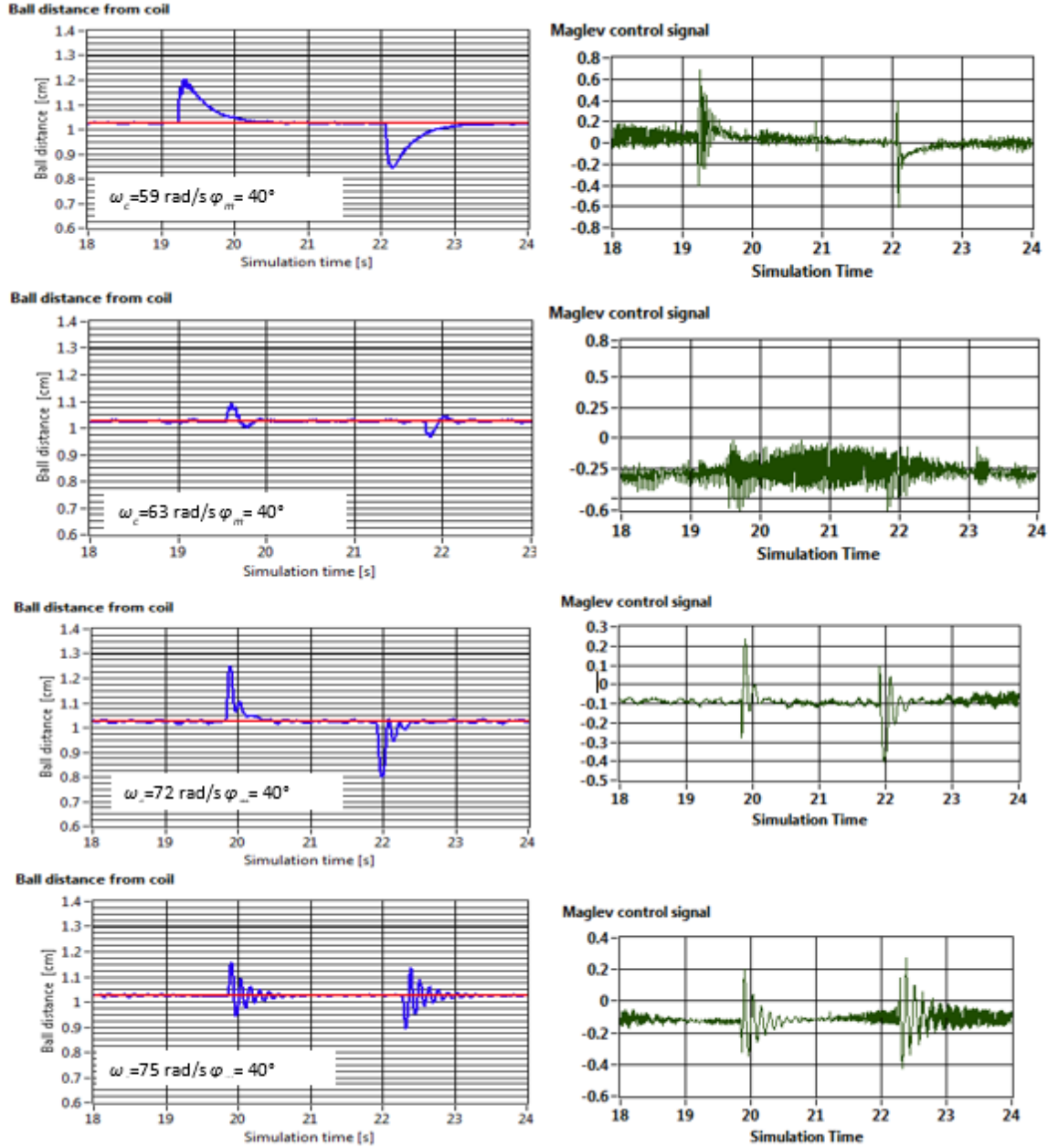


Figure 3.10: System disturbance rejection with different ω_c s by FOPID

From the disturbance rejection results, it can be seen that the FO PID controllers have better disturbance rejection effect to the Maglev system. With FO PID controllers, as ω_c increases the Maglev system has better response to disturbances and less overshoot. Therefore, the advantage of the FO PID controller in improving stability margin and it is also efficient for the low frequency disturbance rejection of the Maglev system.

Considering the similarity between the experimental and simulation results, the simulation herein is omitted and the experimental results will be presented in this section.

Next the disturbance rejection with constant gain cross over frequency and different phase margin.

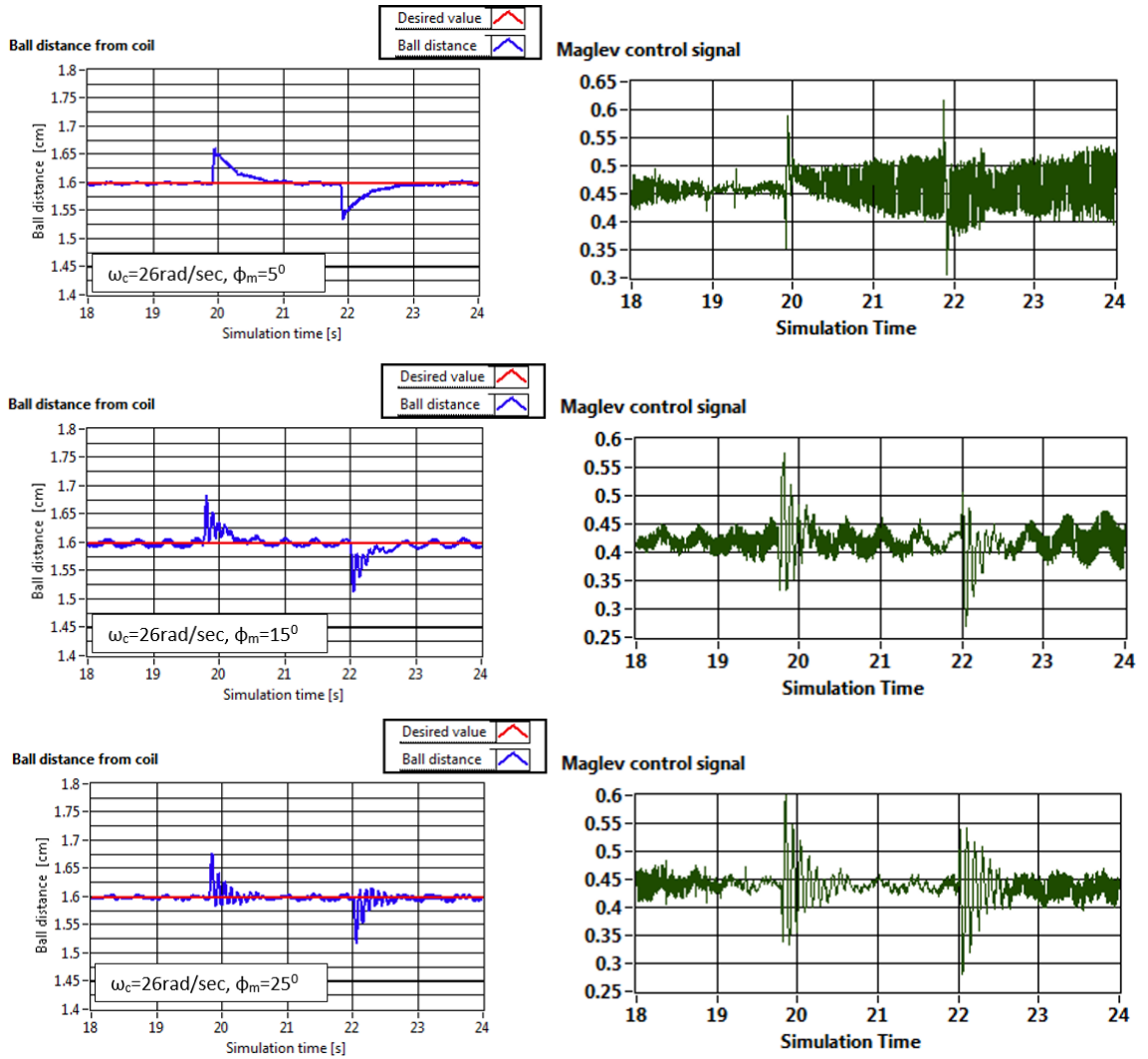


Figure 3.11: System disturbance rejection with different ϕ_m by IO PID

Figures. 3.9,3.10,3.11,3.12, respectively show the experimental results of disturbance rejection with the ϕ_m and ω_c variations. From the results obtained, the Maglev system with FO PID controller has much better disturbance rejection effect as compared to that of IO PID controller.

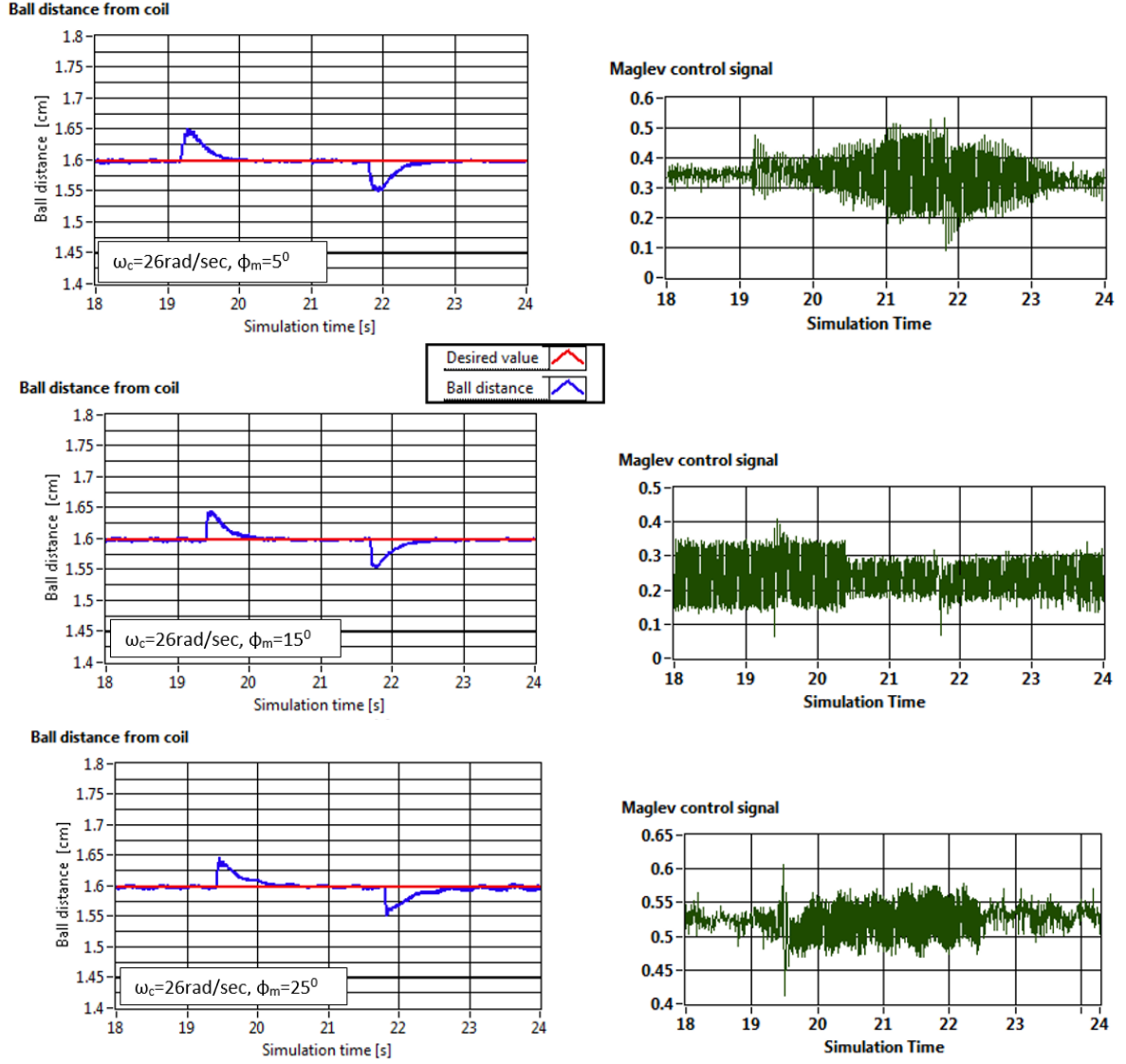


Figure 3.12: System disturbance rejection with different ϕ_m by FO PID

For the FO PID controller, as ω_c increases, the Maglev system has a smaller overshoot and a faster response to the disturbance. In contrast, through a larger ϕ_m slightly enlarges the overshoot and slows the response speed, it is helpful to reduce oscillation. Therefore, the advantage of the FO PID controller in improving the stability margin and closed loop bandwidth is also significant for the low frequency disturbance rejection of the Maglev system.

3.5 TRAJECTORY TRACKING

This section is implemented for showing the efficiency of the suggested FO PID controller compared to IO PID controller. The simulation and experimental validation on Trajectory tracking is carried out in the following sections.

3.5.1 Simulation Result

The simulation results for various trajectory tracking are shown in fig. 3.13–3.15 and their corresponding control signals in fig. 3.14–3.16

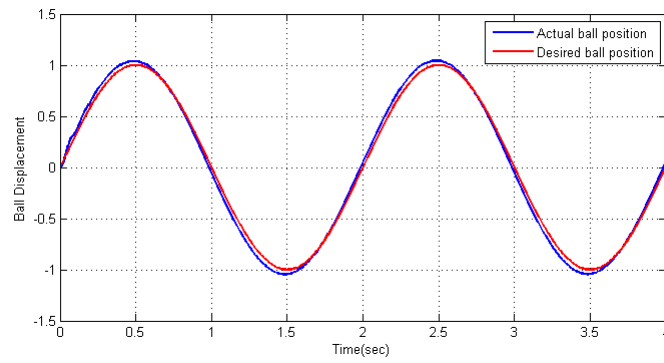


Figure 3.13: Sine wave tracking

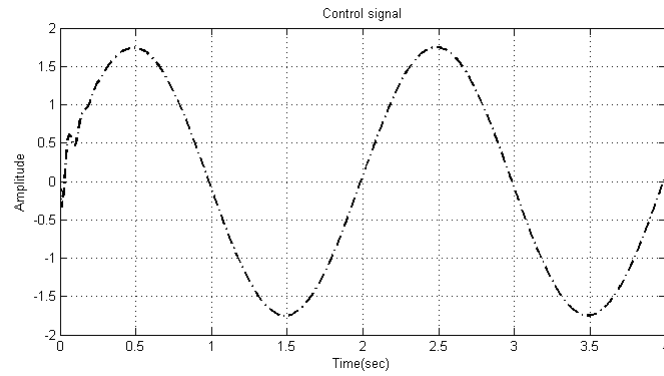


Figure 3.14: Control signal for sine wave tracking

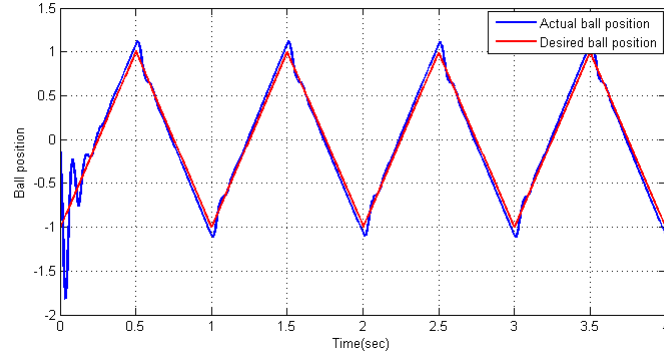


Figure 3.15: Triangular wave tracking

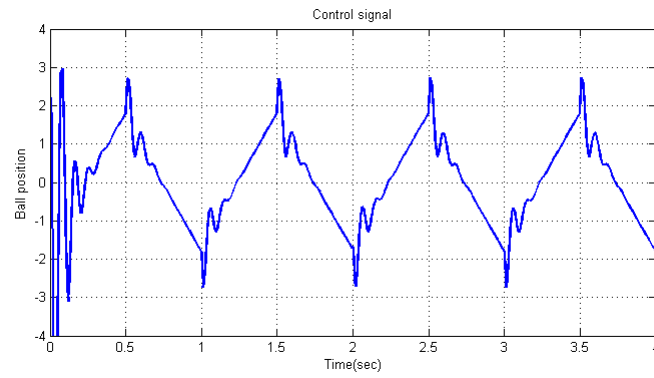


Figure 3.16: Control signal for Triangular wave tracking

3.5.2 Experimental Result

The response of the Fractional Order PID controlled Maglev system in following various trajectories namely sine wave and triangular wave are shown in fig. 3.17 and fig. 3.19 respectively. The control signals corresponding to each trajectory tracking are shown in fig. 3.18 and fig. 3.20.

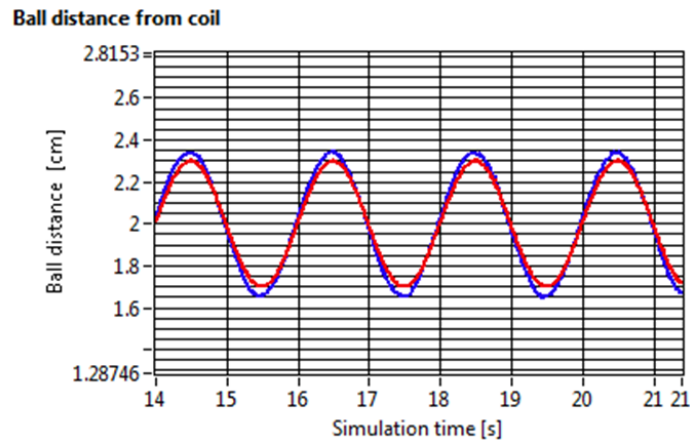


Figure 3.17: Sine wave tracking

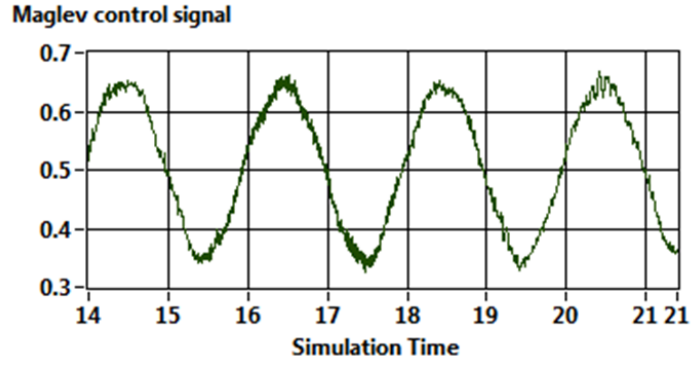


Figure 3.18: Control signal for sine wave tracking

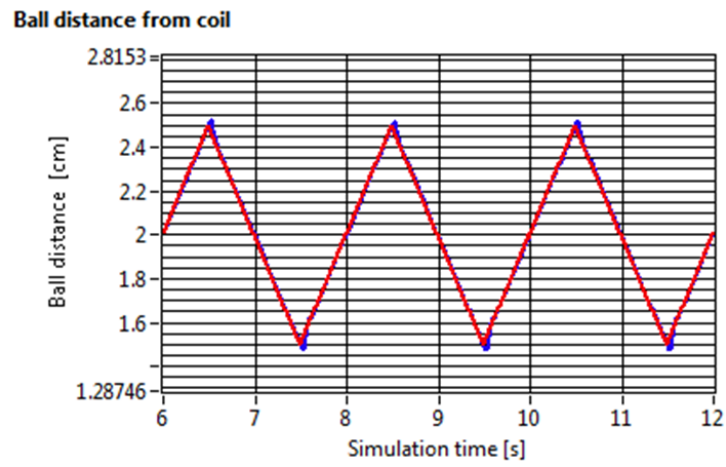


Figure 3.19: Triangular wave tracking

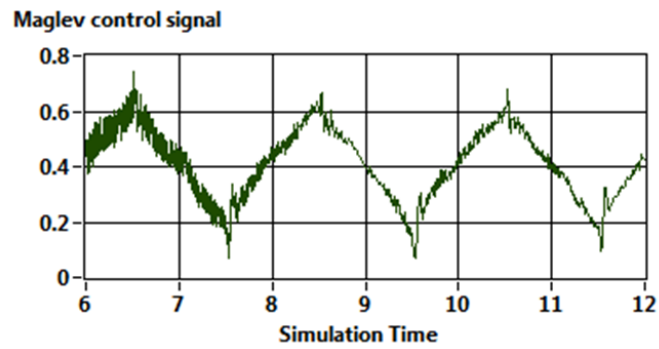


Figure 3.20: Control signal for triangular wave tracking

From the above experimental results, it can be seen that the Maglev system designed using FO PID controller is able to track various reference signals such as step, sine and triangular waves. Also it has good disturbance rejection capability as is evident from fig. 3.10.

3.6 ROBUSTNESS ANALYSIS

3.6.1 Robustness against Loop gain variation

To compare the robustness, the second group of controllers is selected to present the unit step responses of systems with 10% and 20% gain variations (i.e., from $0.8K_t$ to $1.2K_t$). The simulation and experimental validation on robustness against loop gain variation is shown in following sections.

Simulation Result

Fig. 3.21–3.22 shows the system step response with gain variation. It is obvious that the overshoots do change as the gain varies, which is different from the cases in IO PID and FO PID. As for the reason, the differences in model, controller, and specifications may affect the robustness. In addition, the ω_c variations due to the gain variations have a strong effect on overshoots, though ϕ_m has few variations. Anyway, for the unstable system, this shows that the robustness to the gain variations is limited to a small range though the flat phase is guaranteed.

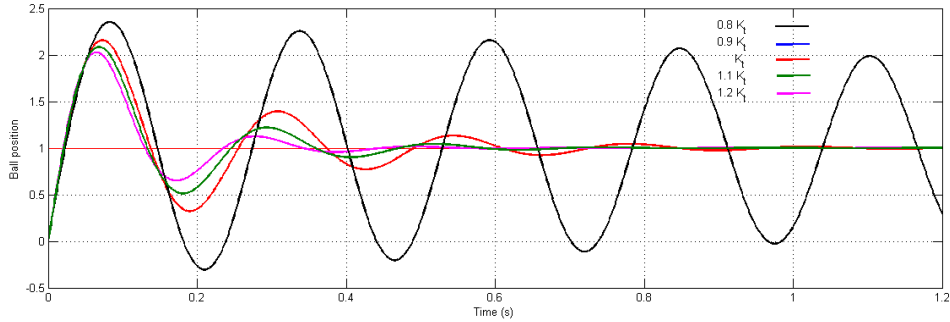


Figure 3.21: Robustness against gain variation by IO PID controller($\omega_c = 24\pi$ and $\phi_m = 20$ deg)

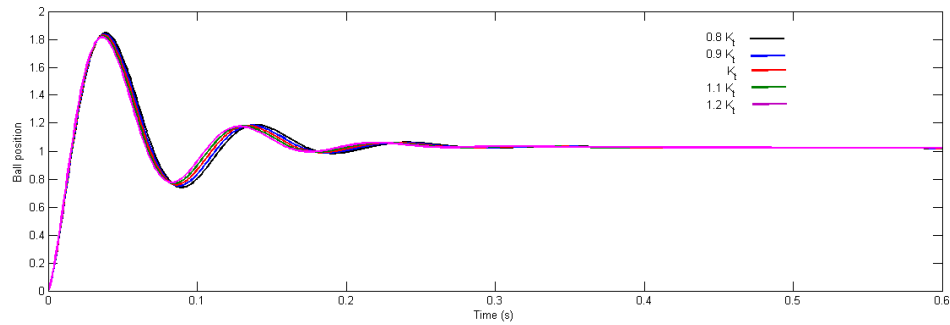


Figure 3.22: Robustness against gain variation by FO PID controller($\omega_c = 24\pi$ and $\phi_m = 20$ deg)

Though the overshoots have changed, the Maglev system with FO PID controllers has much better robustness than that with IO PID controllers from fig. 3.21–3.22, especially for the larger gain variation (the Maglev system with the IO PID controller is unstable when the gain is $0.8K_t$).

Experimental Result

The experimental results of robustness to gain variation are presented in fig. 3.23-3.24. It is obvious that the experiments and simulation have the similar results. In most cases, the system with FO PID controller has better dynamic performance and robustness to gain variations. In addition, the FO PID controller can increase the stability margin and the closed-loop bandwidth, which will be essential to the active control of the Magnetic levitation system.

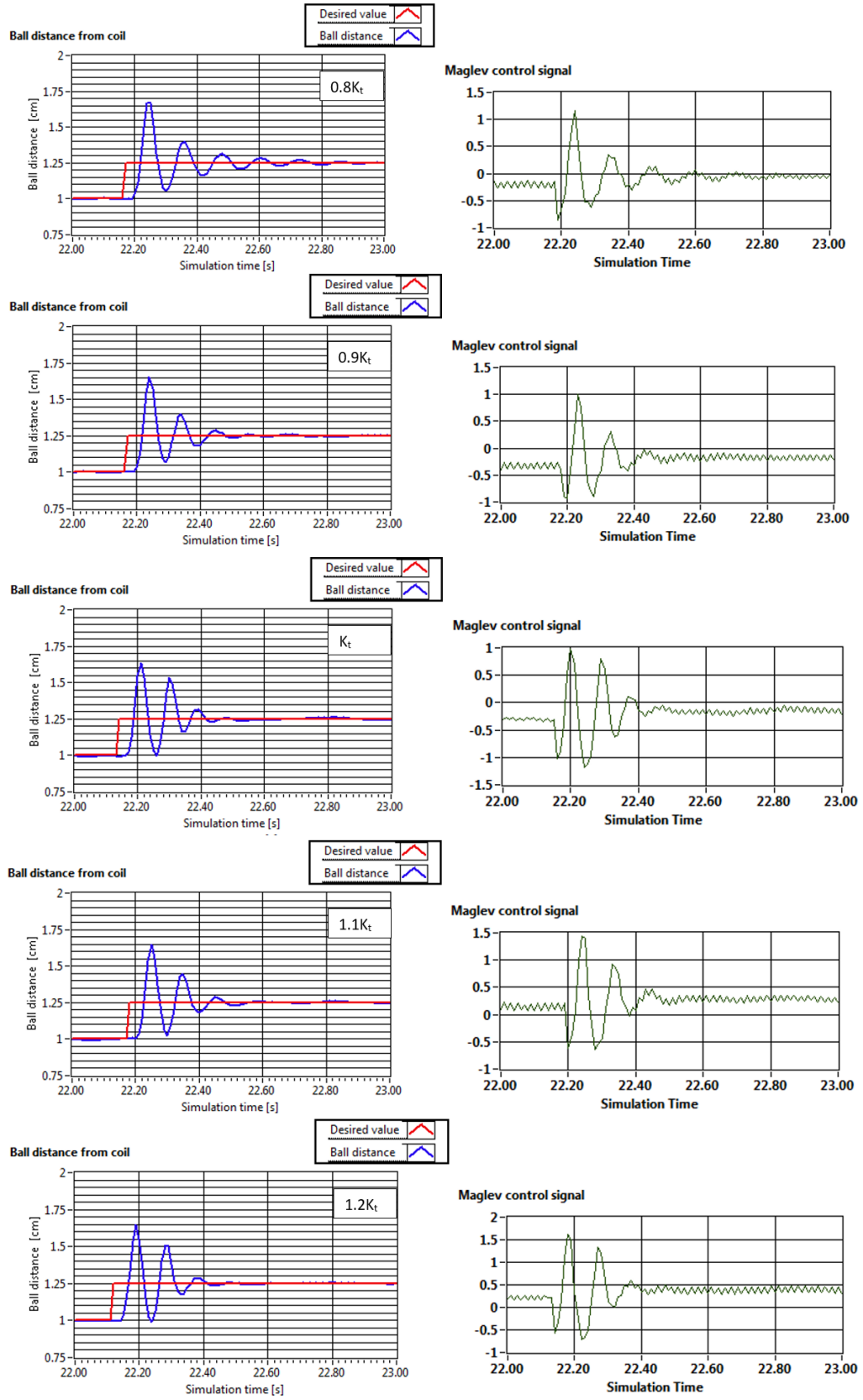


Figure 3.23: Robustness against gain variation by IO PID

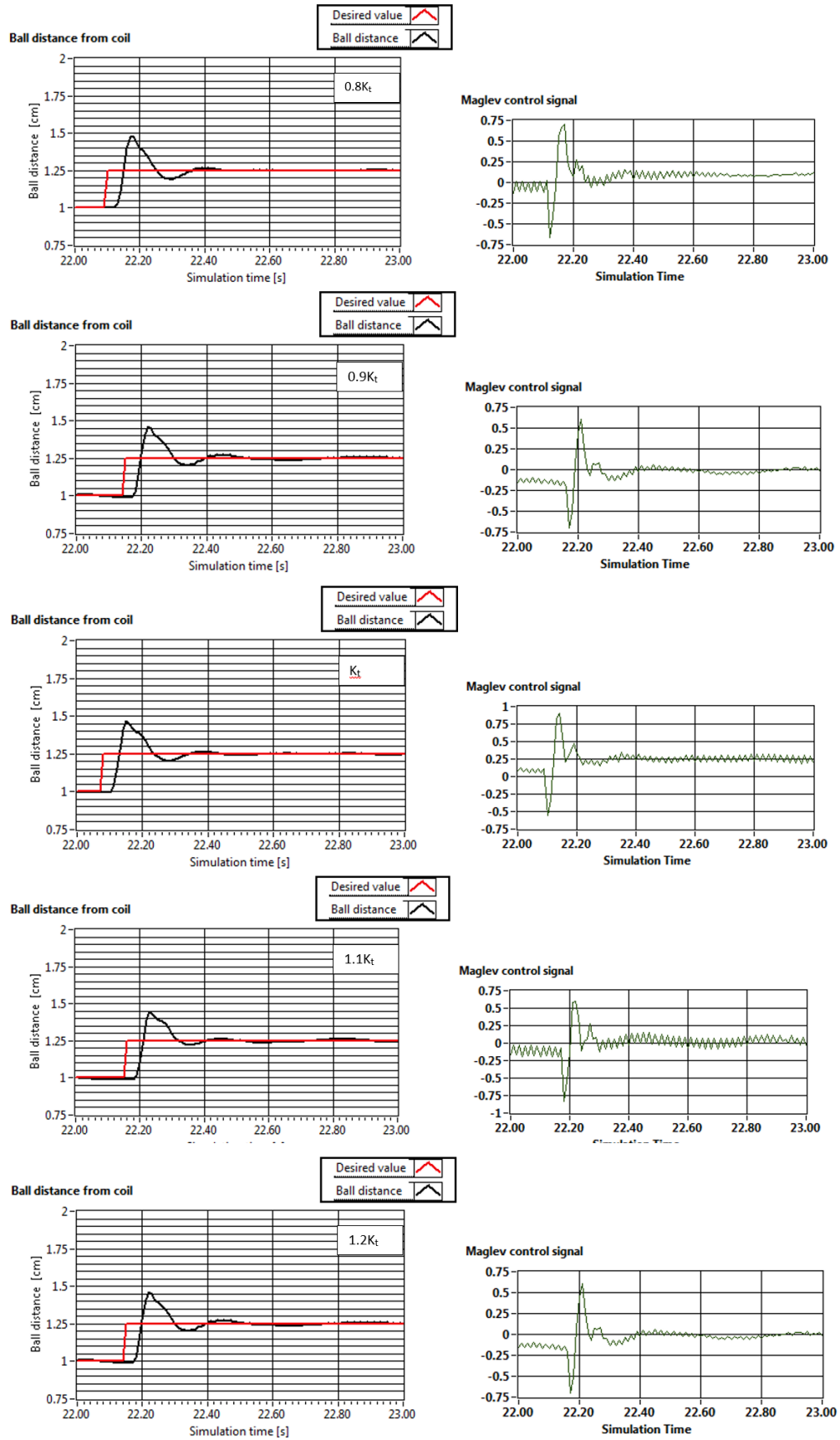


Figure 3.24: Robustness against gain variation by FO PID

3.6.2 Robustness analysis by considering several operating points

To test the robustness of the designed controller, several reference step changes were considered.

Simulation Result

By considering several operating points, the simulation results with regard to robustness is shown below. The responses for various reference input changes are shown in Fig. 3.25 – 3.26.

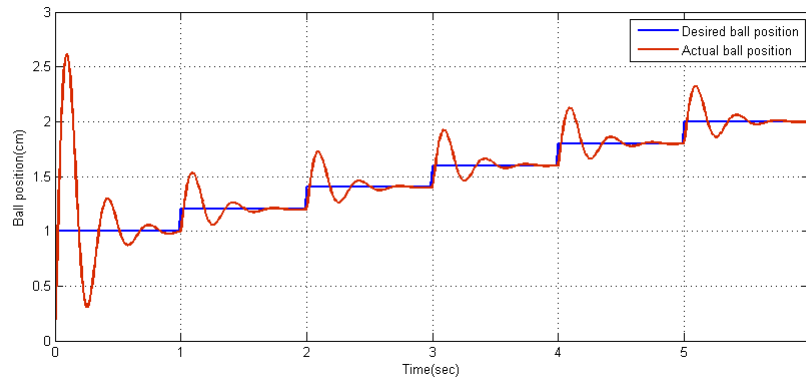


Figure 3.25: Robustness simulation results considering several operating points using IO PID controller

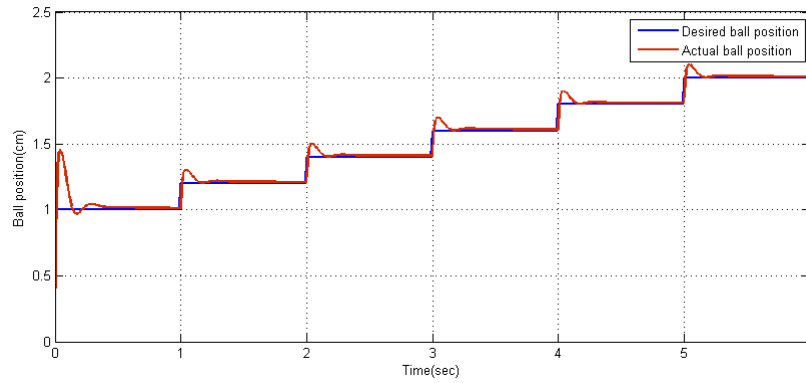


Figure 3.26: Robustness simulation results considering several operating points using FO PID controller

Experimental Result

By considering several operating point the experimental results results regarding with robustness is shown below. The responses for various reference input changes are shown in Fig. 3.27 – 3.28. The corresponding control signals are also shown in Fig. 3.29–3.30

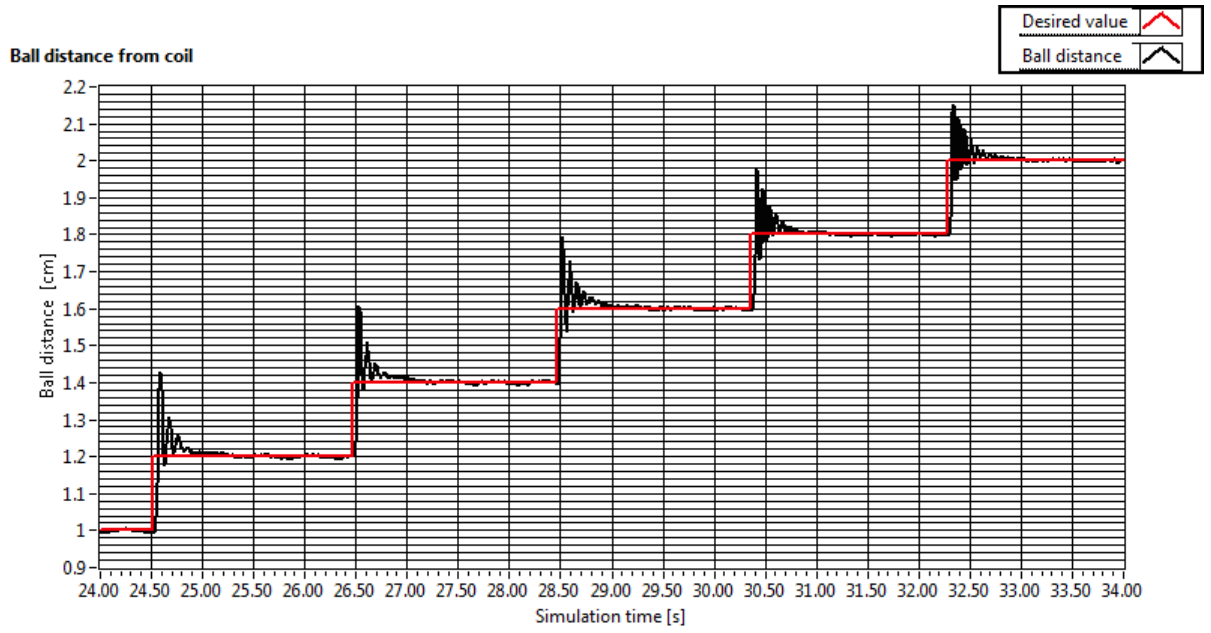


Figure 3.27: Robustness experimental results considering several operating points by the IO PID controller

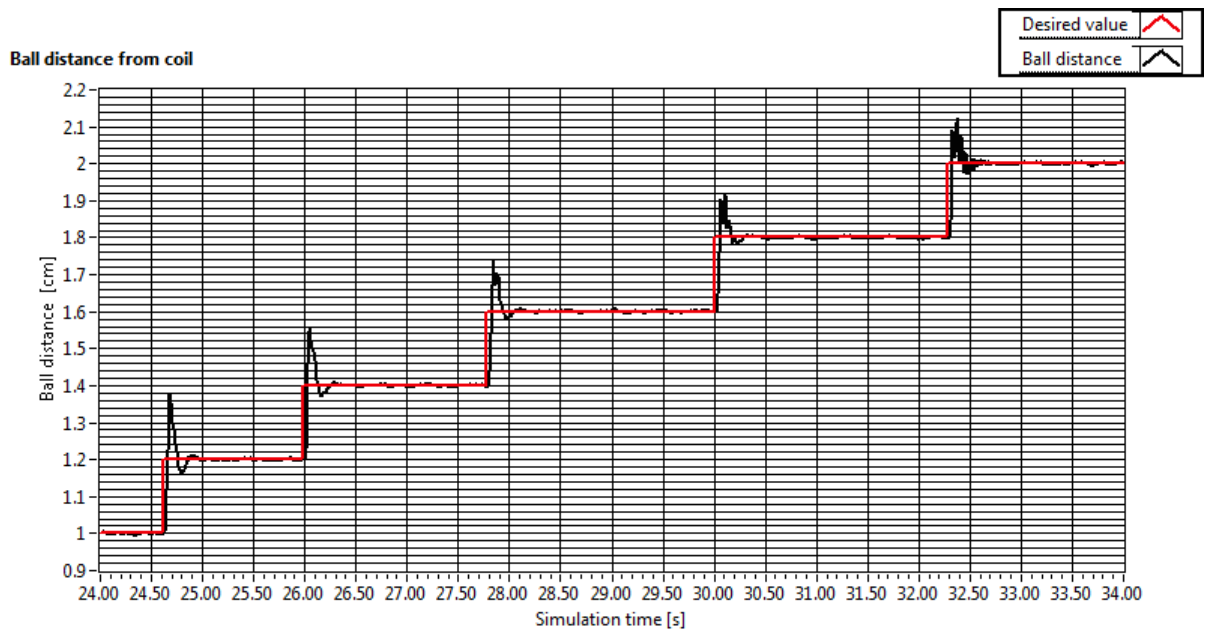


Figure 3.28: Robustness experimental results considering several operating points by the FO PID controller

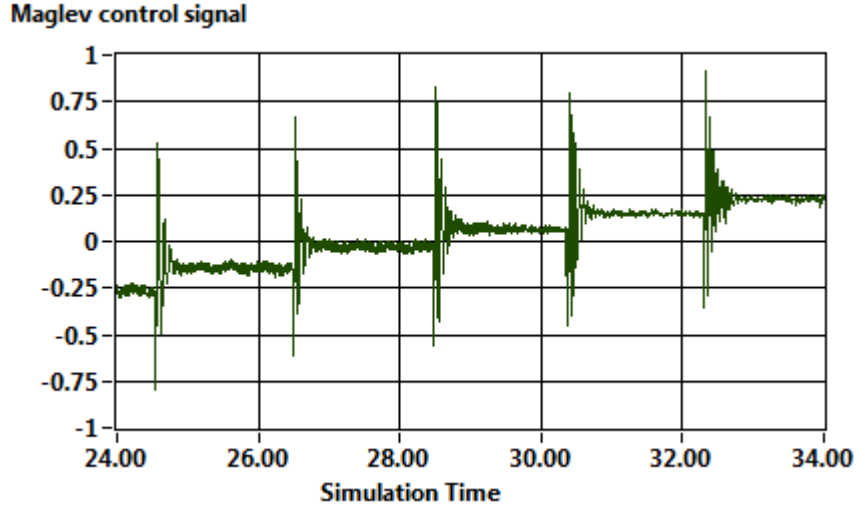


Figure 3.29: Control signals for Robustness analysis by considering several operating points by the IO PID controller

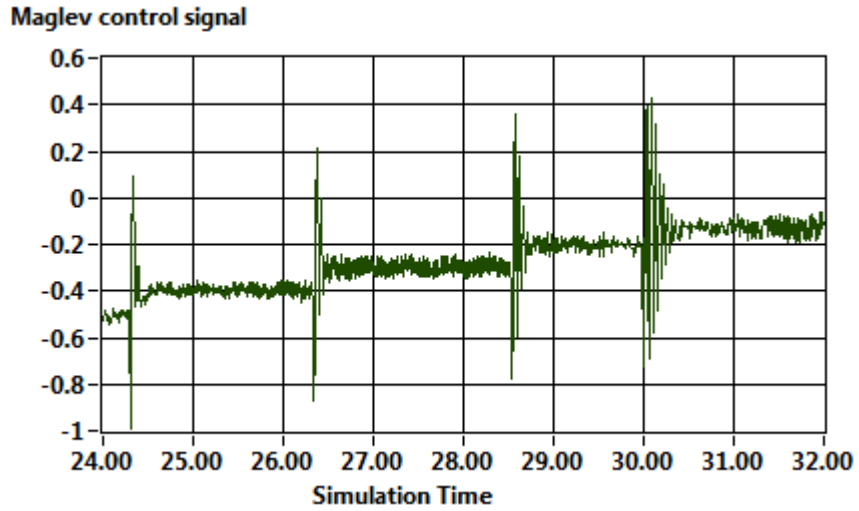


Figure 3.30: Control signals for Robustness analysis by considering several operating points by the FO PID controller

The robustness simulation results considering several operating points given in Fig. 3.27 show a poorer closed-loop performance when compared with the results in Fig. 3.28 obtained with the proposed FO PID controller. The magnetic levitation system experiences some increased oscillations and a larger overshoot when controlled with the IO PID, especially away from the linearization point. The integer order PID provides a poorer robustness compared with the FO controller.

3.7 SUMMARY

The FO PID controller is designed for an IO Maglev system to improve the system stability and dynamic performance. A new numerical search method is proposed for tuning the FO PID controller. Comparing with the previous numerical tuning methods, this method decreases the difficulty in solving the non-linear optimization problem. Both simulation and experimental results demonstrate that the proposed method is effective and the FO PID controller can better improve the system stability and dynamic performance due to the introduction of two more parameters (i.e., λ and μ).

CHAPTER 4

CONCLUSION

This project presents the design and experimental validation of Fractional Order PID controller on a Maglev system using LabVIEW. Design is based on a set of performance specification such as phase margin, gain cross over frequency and robustness to gain variation in plant. Experimental results demonstrate the ability of the controller in tracking various reference signals and rejecting the constant disturbances. Also, the Fractional Order PID controlled Maglev system exhibits good dynamic performances and improves system stability. A comparison with the existing PID controllers is made which confines the superiority of the proposed method. Comparing with the IO PID controller, though the FO PID controller is more complicated in practical applications, the improvement in system performance confirms that this cost is worthwhile.

SCOPE FOR FUTURE WORK

In future work, build a fractional order cooperative control system using multiple LabVIEW hardware in the loop platforms. To cooperate two systems each other, the communication is a very important issue. Fortunately, LabVIEW provides some networking features to share data with other VIs over the network, and it can also communicate with other applications and VIs through low level communication protocols. So use LabVIEW as a client to subscribe the data and use features in other applications. Specifically, the National Instruments Data Socket technology is a good way for us to build cooperative motion control system platform. Data Socket connection of LabVIEW allows us to write and read data through URL which just like URLs in a web browser. Therefore, just specify a server, so others can read data from the server or write data to the server which makes it convenient to transfer data between two machines.

Actually, LabVIEW also can connect with MATLAB/Simulink. Matlab/Simulink can work with RTW (Real-Time Workshop) to test and develop advanced control algorithms. However, Simulink is lack of the virtual instruments to operate, so the LabVIEW connecting with MATLAB/Simulink should be very practically attractive. The Simulation Interface Tool-kit is a module provided by LabVIEW. The Tool-kit enables LabVIEW to run and communicate with Simulink based on the internet connection.

PUBLICATIONS

The paper titled “**LabVIEW based real time implementation of Fractional Order PID controller for a Magnetic levitation system**” is to be presented at *IEEE First International conference on Power electronics, Intelligent control and Energy systems 2016*, Delhi Technical University

REFERENCES

- [1] N.F. AL-Muthairi , M. Zribi, “Sliding Mode Control of a Magnetic Levitation system”, *Mathematical Problems in Engineering*, pp.93-107.2004
- [2] Walter Barie, John Chaisson, “Linear and nonlinear state space controllers for magnetic levitation,” *International Journal of Systems science*, Vol. 27, pp. 1153-1163, 1996.
- [3] A. El Hajjaji and M. Ouladsine, “Modeling and nonlinear control of magnetic levitation systems,” *IEEE Transactions on Industrial Electronics* 48, no. 4, pp. 831 838, 2001.
- [4] A. Charara, J. DeMiras, and B.Caron, ”Nonlinear control of a magnetic levitation system without premagnetization,” *IEEE Transactions on Control Systems Technology* 4 , no. 5, pp. 513 523, 1996.
- [5] M. R. Filho and C. J.Munaro, “A design methodology of tracking controllers for magnetic levitation systems,” *IEEE International Conference on Control Applications*, (Mexico City), pp. 47 51, 2001.
- [6] D.Valerio and J. Se da costa, “A review of tuning methods for fractional PIDs,” *Proc. 4th IFAC Workshop Fract. Differ. Appl.* , Badajoz, Spain,pp. 1-5,2010.
- [7] B. M. Vinagre Jara,“Modelado y control de sistemas caracterizados por ecuaciones Ántegro-diferenciales de orden fraccional,” (in Spanish), Ph.D. dissertation, Univ. Nacional Edu. Distancia, Madrid, Spain, 2001.
- [8] Y. Q. Chen, H. Dou, B. M. Vinagre, and C. A. Monje,“A robust tuning method for fractional order PI controllers,” *Proc. 2nd IFAC Workshop Fract. Differ. Appl*, Porto,Portugal,pp. 1-6.
- [9] H. Li, Y. Luo, and Y. Q. Chen, “A fractional order proportional and derivative (FOPD) motion controller: Tuning rule and experiments,” *IEEE Trans. Control Syst. Technol.* , vol. 18, no. 2, pp. 516-520, Mar. 2010.
- [10] Y. Q. Chen, T. Bhaskaran, and D. Xue, “Practical tuning rule development for fractional order proportional and integral controllers,” *Proc. ASME International Design Engineering Technical Conferences , Computers and Information in Engineering Conference* 2007.

- [11] Jianpeng Zhong and Lichuan Li, "Tuning Fractional-Order PID Controllers for a Solid-Core Magnetic Bearing System," *IEEE transactions on control systems technology*, vol. 23, no. 4, July 2015.
- [12] Ravi Kumar Jatoth Venu Kishore K,Nagu.Bhookya "A Comparative Study on Design and Tuning of Integer and Fractional Order PID Controller," in *Proc.Int. Conf. on Modelling, Identification and Control*, Melbourne, Australia, December 3-5, 2014
- [13] WANG Chunyang, FU Weicheng, SHI Yaowu , "Tuning Fractional Order Proportional Integral Differentiation Controller for Fractional Order System," *proceeding of 32nd Chinese control conf* ,July 26,2013
- [14] Silviu Folea, Cristina I. Muresan, Robin De Keyser, and Clara M. Ionescu, "Theoretical analysis and experimental validation of a simplified fractional order controller for a magnetic levitation system," *IEEE Transaction on Control Systems Technology*, vol. 24, no. 2, March 2016.
- [15] Vinodh Kumar Ea, Jovitha Jeromeb,"LQR based optimal tuning of PID controller for trajectory tracking of Magnetic Levitation System," *International Conference On Design and Manufacturing*, IConDM 2013.